REPORT DOCUMENTATION PAGE

Form Approved
OMB No. 0704-0188

1. AGENCY USE ONLY *(Leave blank)*	2. REPORT DATE	3. REPORT TYPE AND DATES COVERED
	September 15, 2000	Final Report, September 1999 - August 2000

4. TITLE AND SUBTITLE
Real-time hydrometeorological forecasting and analysis from radar and satellite observations

5. FUNDING NUMBERS
Army Research Office
(DAAD19-99-C-0051)

6. AUTHORS
Ross N. Hoffman

7. PERFORMING ORGANIZATION NAME(S) AND ADDRESS(ES)
Atmospheric and Environmental Research, Inc.
840 Memorial Drive
Cambridge, MA 02139

8. PERFORMING ORGANIZATION REPORT NUMBER
P-871-RP-I-00

9. SPONSORING/MONITORING AGENCY NAME(S) AND ADDRESS(ES)
U.S. Army Research Office
Attn: AMSRL-RO-RI (Sylvia Hall)
PO Box 12211
Research Triangle Park, NC 27709-2211

10. SPONSORING/MONITORING AGENCY REPORT NUMBER
ARO 40220.1-EV-ST1

11. **The views, opinions and/or findings contained in this report are those of the author(s) and should not be construed as an official Department of the Army position, policy or decision, unless so designated by other documentation.**

12a. DISTRIBUTION/AVAILABILITY STATEMENT
Approved for public release; distribution unlimited.

12b. DISTRIBUTION CODE

13. ABSTRACT *(Maximum 200 words)*

Our approach provides a flexible, realistic, low-risk, integrated approach to precipitation and hydrological forecasting. This approach: (a) exploits the enhanced capability of the NEXRAD system to provide accurate high-resolution rainfall maps over the continental U.S.; (b) utilizes state-of-the-art precipitation and hydrological forecasting techniques; but (c) overcomes the inherent limitations of these approaches by optimally merging the results of the different techniques to provide a robust solution.

River forecasting has many uses and benefits. Floods affect civilian populations, Army Corps operations, mobility, forward army units, and others. River management optimizes the use of water for drinking, agriculture, hydroelectricity, navigation and environmental quality control.

14. SUBJECT TERMS
River flow; NEXRAD; weather radar, precipitation, hydrometeorological; hydrological; modeling; analysis

15. NUMBER OF PAGES
61

16. PRICE CODE

17. SECURITY CLASSIFICATION OF REPORT	18. SECURITY CLASSIFICATION OF THIS PAGE	19. SECURITY CLASSIFICATION OF ABSTRACT	20. LIMITATION OF ABSTRACT
Unclassified	Unclassified	Unclassified	Unlimited

Atmospheric and Environmental Research, Inc.

840 Memorial Drive
Cambridge, Massachusetts
02139-3771

Telephone
617 547-6207

Facsimile
617 661-6479

www.aer.com

Final Report

ARO DAAD19–99–C–0051

AER P871

Real-time hydrometeorological forecasting and analysis from radar and satellite observations

A Phase 1 STTR Project for Topic
ARMY99T004

Submitted to
U.S. Army Research Office
ATTN: Dr. Russell S. Harmon
P. O. Box 12211
Research Triangle Park, NC 27709-2211

Submitted by
Atmospheric and Environmental Research, Inc.
September 15, 2000

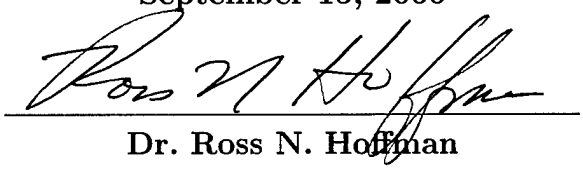

Dr. Ross N. Hoffman
Principal Investigator
rhoffman@aer.com

Contents

1 Scope

1.1 Identification

This document constitutes the final technical report of Phase I for AER Project 871 (P871) on "Robust weather radar algorithms for hydrometeorological forecasting and analysis" funded by the Army Research Office (DAAD19–99–C–0051).

The reporting period is September 1999 through September 2000.

1.2 System Overview

1.2.1 Objectives of the Project

The primary objective of P871 is to develop and implement a state-of-the-art system for hydrometeorological and hydrological forecasting, which we call the Rain and River Forecast System (R^2FS).

River forecasting has many uses and benefits. Floods affect civilian populations, Army Corps operations, forward army units, and others. Flash-flood events, the 1993 midwest river flooding, and the recent flooding in western and upper midwestern states are reminders of the havoc that extreme hydrometeorological events can cause. Floods and flash-floods are the leading realization of weather hazards. Deaths and damage by floods are in excess of those by lightning, tornadoes, and hurricanes. Predictions of flood stage and soil moisture fields have additional applications in mobility and ground deployment planning.

Clearly, the technology developed under this topic will have broad applicability to government and private sectors. Furthermore, longer-lead forecasts also benefit water resources, reservoir control, and river navigation management activities. As population and pollution increase, clean, fresh water becomes an increasingly prized resource. Rivershed management tools, such as R^2FS, will find ever widening applications, both in the U.S. and in other parts of the world.

1.2.2 Major Functions

The prototype R^2FS system developed during Phase I integrates the functions of pre-existing modules to produce high quality precipitation estimates from NEXRAD and NWP forecasts and to use these to drive the physically based hydrological forecast. These modules include:

PRECIP: The WSI mosaics of NEXRAD precipitation.

Eta: The NCEP regional scale NWP model.

CASC2D: The U. Conn. distributed-parameter hydrologic model.

WMS: Graphical interface to CASC2D and other hydrologic models.

The use and integration of these system modules has provided a working prototype for model testing and comparison during Phase II, which will included model development plans that build upon and improve the existing prototype.

1.3 Document overview

This document reports the development of the prototype Rain and River Forecast System (R^2FS) during the Phase I project effort.

We begin with an introduction describing the opportunities and issues that motivate our approach (§ 2). Then we describe our overall approach to the problem in § 3. The final results from the Phase I effort are summarized with respect to precipitation in § 4.2 and with respect to hydrology in § 4.3.

2 Introduction

This project for "Robust real-time distributed hydrometeorological forecasting and analysis from radar and satellite observations" is a collaboration between Atmospheric and Environmental Research, Inc. (AER) and the Ralph M. Parsons Laboratory of the Civil Engineering Department of the Massachusetts Institute of Technology (M.I.T. Parsons), with the cooperation of the Massachusetts Institute of Technology Lincoln Laboratory (M.I.T. Lincoln Lab), and Weather Services International Corporation (WSI). The "Rain and River Forecast System" (R^2FS) that we are developing is built on integrating: 1) multi-source weather sensing including NEXRAD radar, 2) a suite of tested data quality-control and interpretation procedures, and 3) advanced distributed hydrological models for complex terrain. The distinguishing features of the project are the approaches to data fusion and system integration (Fig. 1). Specifically, the skillful extension of the hydrological prediction lead-time, by including robust quantitative precipitation forecasting capability within the framework of the system, is a key component of the proposed project. The team includes technical expertise and experience for the implementation of the key components of the project. The team leaders are Dr. Hoffman of AER, and Prof. Entekhabi of M.I.T. Parsons. Dr. Hoffman is an expert in the use of remotely sensed data for NWP. Prof. Entekhabi is an expert in hydrological modeling. The project also included cooperation with M.I.T. Lincoln Lab for short-term precipitation forecasting using feature tracking, and from WSI for the analysis of precipitation from NEXRAD.

Modern approaches to precipitation estimation and hydrological forecasting have the potential to provide significant improvements in flood hazard mitigation through advanced warning. The forecast of flash-flood potential and river flooding requires the integration of precipitation estimates and distributed hydrological models. Precipitation is the ultimate source of all water in a river. Hydrological models simulate the processes by which precipitation is stored and transmitted in a river basin. These processes include evaporation, infiltration, percolation, runoff, and subsurface flows, and, in some climate regimes, snowpack accumulation and snow melt. Clearly, to forecast river flow is a complex problem.

From a physical point of view, river flow depends on the upstream topography and soil characteristics; the initial ground water, soil moisture, snow cover, and river stage; and the precipitation (Fig. 2). In flood situations these are the controlling factors, but in general, evaporation must also be modeled. Additional requirements are therefore forecasts of the moisture, temperature, and wind speed just above the ground and the temperature of the surface. All these factors must be estimated for modern, state-of-the-art distributed hydrological modeling. The most important factor is usually the forecast precipitation, although in special situations the factors contributing to snow melt can be the most important.

A major problem facing operational precipitation and flood forecasting is the incompatibility of the hydrometeorological forecast data products with the requirements of flood forecasting. The skill associated with flood hydrograph or flash-flood forecasts is critically dependent on the precipitation input at high spatial and temporal resolution; in flood situations, the hydrology model is essentially only partitioning the precipitation into runoff and infiltration. Quantitative Precipitation Forecast (QPF) may be used to extend the lead-time of hydrological forecasts. Current QPF procedures are however not well-suited for many hydrological applications because they have been developed with focus on areal coverage at regional scales rather than amount (especially at higher intensities) at basin scales.

The recently commissioned national network of Doppler weather sensing radars (WSR-88D units owned and operated by NOAA, DOD, and FAA, hereafter referred to as NEXRAD) provide data with unprecedented space-time resolution of precipitation storm structure and amount. The development and testing of robust operational radar algorithms for all types of hydrometeorological regimes (convective rainfall, stratiform precipitation with bright-band, snow, etc.) is now fairly mature. Over the last few years there have been major advances in processing the NEXRAD data. We use NEXRAD precipitation estimates produced operationally in real-time by WSI. This product is compared favorably to gauges in § 4.2, and has previously been validated by Vollrath (1996 [49]).

In addition to NEXRAD nowcasting, the impact of quantitative precipitation and temperature forecasts on longer lead hydrological predictions of streamflow and flood crest is crucial. Therefore, a requirement exists for improved gridded quantitative precipitation forecasts (QPF) with time-resolution and for lead-times, that are consistent with hydrological applications. A major component of the activities for this project is the development of a QPF system that is capable of ingesting multiple weather sensing systems and incorporating the best features of different predictive models at various lead-times. For example, for small basin flash-flood events the time range is 0 to 6 hours and for larger basin main-stem flooding events the time range is 0.5 to 3 days.

The approach to robust QPF determination is to merge or fuse forecasts derived using various tools and techniques, weighting the individual estimates depending on their accuracy as a function of lead-time. In this manner the best features of each technique are integrated, thereby extending the lead-time of hydrological forecasts. In the short-term, extrapolation of current observed conditions possess some skill. The proposed QPF system will use, as precipitation estimates up to the present time, mosaics of WSR-88D estimates (the WSI PRECIP product described in § 3.1). These estimates of the precipitation field will then

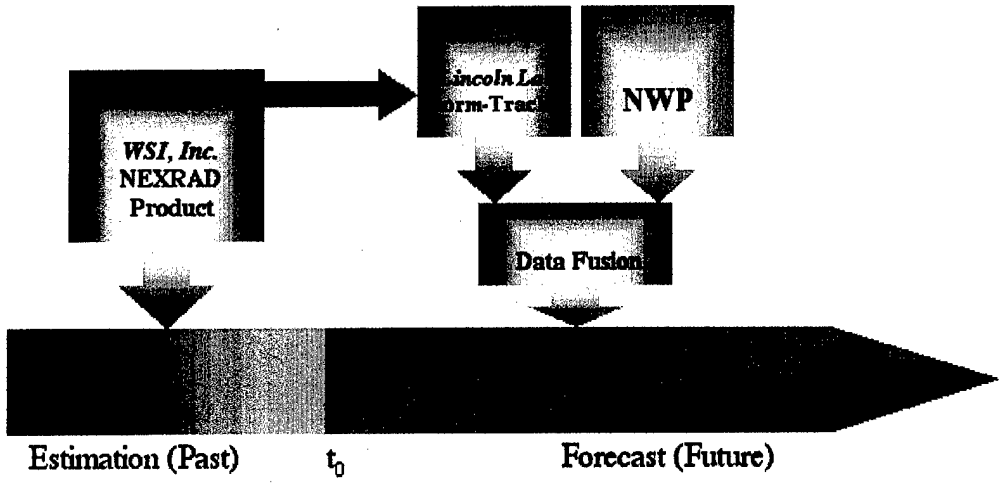

Figure 1: The R^{2}FS data flow for the QPF component. Before the forecast starts at time t_0, the observed radar precipitation is assimilated by the hydrological model. The radar data is also used by the storm tracker to extrapolate the precipitation pattern. This forecast is merged with the NWP forecast, with weight varying with forecast time.

be extrapolated using an advection algorithm based on a timelapse correlation technique developed for the FAA at M.I.T. Lincoln Lab. The skill of this contribution to the QPF will be very good for very short lead-times up to 30 minutes, but it will rapidly deteriorate as the lead-time is increased beyond one hour. (See Fig. 3.) For longer lead-times, we propose to use NWP precipitation fields. In addition, other fields needed to model evaporation will be provided by the NWP model.

The current generation of operational hydrometeorological forecasting procedures and real-time hydrological prediction models are incapable of taking advantage of the full information content of current radar observations. Conceptual hydrological models used in operational settings are derived from empirical frameworks developed over thirty years ago (NRC 1996 [34]). These lumped models were designed to work with sparse point observations by rain gauges. New and innovative spatially-distributed hydrological models and hydrometeorological assimilation procedures are needed to realize the full potential of the modern observation networks.

The new generation of hydrological models is based on digital topographic data. The Army's Waterways Experiment Station (WES) has invested considerable resources in the CASC2D distributed watershed model, and the Watershed Modeling System (WMS) hydrological model interface (§ 3.5). CASC2D solves the equations of conservation of mass and momentum to determine the timing and path of runoff in the watershed. Another model of this sort is the M.I.T. Parsons Model. The M.I.T. Parsons Model treats additional physical processes including full infiltration front tracking and groundwater redistribution based on two-way coupled saturated and unsaturated soil zones.

In summary, our response to this opportunity is to propose the development of a "Rain

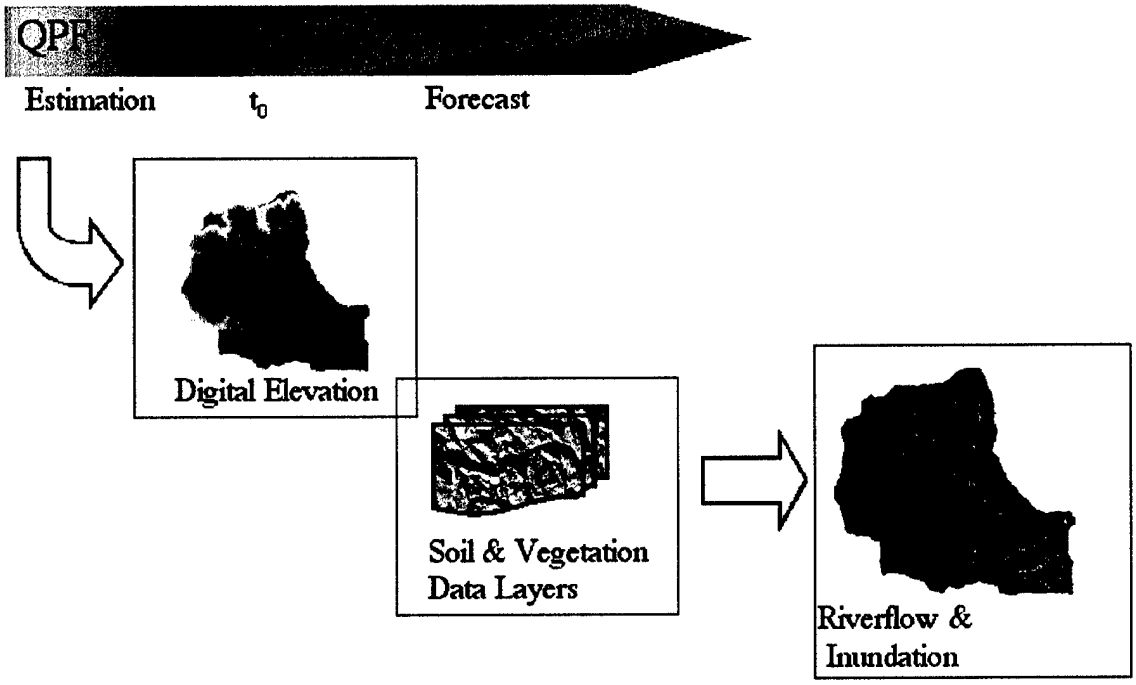

Figure 2: The R^2FS data flow for the river flow component. The precipitation estimates and forecasts are a principal input to the hydrological model. The digital elevation and initial soil moisture modulate the response to the precipitation to produce spatially varying forecasts of riverflow and flooding.

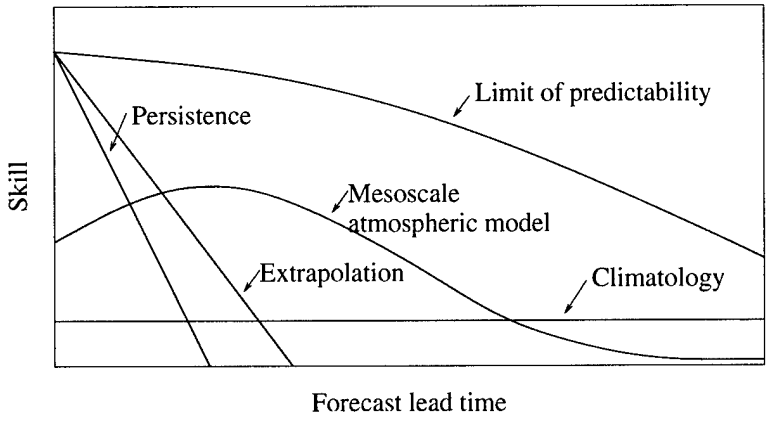

Figure 3: Predictability of precipitation (after Zipser (1990 [56])). At different forecast ranges, different forecast techniques have varying skill. The theoretical limit to predictability is caused by the chaotic nature of the atmosphere. Note that numerical weather prediction models are poor at predicting precipitation at short lead times, because of imbalances between the moisture and mass and momentum initial specifications.

and River Forecast System" (R^2FS). The basic components (schematically illustrated in Fig. 1 and Fig. 2) are precipitation analyses, precipitation forecasts, a distributed hydrological model, and verification tools. The hydrological model should include the effects of melting snow and subsurface flows of water. Baseline, and in some cases operational, versions of these components exist. The ones we propose using are described in § 3. Currently, the weakest link is the precipitation forecast. Our proposal centers around optimizing the use of available precipitation forecasts, and assembling the components into a system in such a way that refinements and improvements can be accomodated in an evolutionary approach.

3 The R^2FS

Our plan for the R^2FS provides a flexible, realistic, low-risk, robust, and integrated approach to precipitation and hydrological forecasting. This approach: (a) exploits the enhanced capability of the NEXRAD system to provide accurate high-resolution rainfall maps over the CONUS; (b) utilizes state-of-the-art precipitation and hydrological forecasting techniques; but (c) overcomes the inherent limitations of these approaches by optimally merging the results of the different techniques. The R^2FS design stresses flexibility, modularity, and extensibility leading to a system with low developmental risk and low operational maintenance costs. The overall R^2FS is depicted in Fig. 1 and Fig. 2. The elements of R^2FS are introduced in the following paragraphs and described in more detail in the subsections that follow. The completion of the working R^2FS prototype during a relatively short period, has demonstrated the possibilty of integrating pre-existing modules into an forecasting system for hydrometeorologic purposes. Improvements to the baseline system during Phase II have been designed by taking into account the key findings from the Phase I effort.

The standard operational NEXRAD products suffer from a number of problems which make them less accurate than is desirable for hydrological forecasting. For example, a single reflectivity to precipitation (Z/R) relationship is used. However, it is known that the Z/R relationship depends in general on the type of situation (e.g., frontal rain, steady widespread rain, convection). The operational NEXRAD products are oriented to a single radar site—coverage for an individual watershed may require a mosaic of several sites. R^2FS will overcome these various problems by using the WSI PRECIP product (§ 3.1). This is a state-of-the-art, value-added, operational NEXRAD rainfall analysis with national coverage. PRECIP is compared favorably to gauges in § 4.2, and has previously been validated by Vollrath (1996 [49]).

No single precipitation forecast technique is optimal for all forecast ranges or synoptic situations. Consequently, R^2FS encompasses a number of techniques and methods of combining them. A number of individual techniques are described in section § 3.2, and methods for blending the individual forecasts are discussed in section § 3.3. Not all individual forecast or blending techniques mentioned in these sections will be immediately implemented in R^2FS—some are too risky, some are too developmentally or computationally expensive, some require unavailable historical data sets. An important aspect of selecting, tuning, and blending precipitation forecast techniques is assessing their accuracy. The R^2FS approach

to precipitation verification is discussed in section § 3.6.

A large number of empirical-physical models of river flow have been proposed as tools for hydrologic modeling. Many are used operationally today for a variety of purposes and in a variety of scenarios. Lumped and conceptual hydrologic models represent a watershed as a small number of interconnected buckets or storages that transmit water flux through certain explicit processes. Modern distributed hydrological models attempt to directly model all relevant physical processes using physically-based equations of mass, momentum and energy conservation. We use the WMS/CASC2D as our baseline hydrological model during Phase I(§ 3.5). CASC2D is a distributed-parameter model for simulating the hydrological response of a watershed subject to an input rainfall field for infiltration-excess or Hortonian flow basins. CASC2D includes the most important physical processes for modeling river flow in regions dominated by the Hortonian runoff production mechanism (i.e. infiltration capacity of the soil is exceeded by the rainfall intensity). WMS is a comprehensive software package for developing computer simulations of watersheds and provides a graphical interface and model preprocessor to CASC2D.

3.1 Accurate, Robust Radar Precipitation

The NEXRAD system has great potential to monitor precipitation. However, current standard precipitation products have a number of problems including a simplified Z/R relationship, bright band effects, range effects, anomalous propagation, and others. The accuracy of the single site, radar-based precipitation estimates is particularly contingent on the choice of the right Z/R relationship. Well over 100 such relationships have been identified in research over the years. The best Z/R relationship is dependent on a number of factors including the nature of precipitation (e.g. convective versus stratiform) and the type of precipitation (drizzle, rain, snow, sleet, hail).

Considerable work by government, university, and for-profit organizations have already produced greatly improved NEXRAD precipitation products. To avoid duplication of effort we will make use of the WSI PRECIP, which is an operational real-time product. The algorithms for WSI PRECIP are proprietary and will not be a project deliverable, but WSI PRECIP is COTS and readily available. Coverage is available over the entire CONUS at 15 minute intervals and at $\sim 2\ km$ resolution. Examples of 3 hour accumulations of PRECIP data are shown in Fig. 4. Cumulative totals appear in color contoured bands.

PRECIP is based on WSI's NOWrad radar mosaics. NOWrad mosaics are quality assured every 15 minutes, 24 hours-a-day, 7 days-a-week using a three-step process that combines automated algorithms and manual review and adjustment by a trained meteorologist. The automated algorithms ensure the latest data is received from all the sites as quickly as possible, and filter out obvious false echoes (large areas or even individual pixels). The final step of quality assurance is done on an advanced workstation: A meteorologist compares the radar mosaic data to other data, including satellite, lightning, surface observations, in order to identify and remove areas of remaining false echoes. The radar mosaic is released on average about 7 minutes after data capture. The compositing of all the radar sites fills in

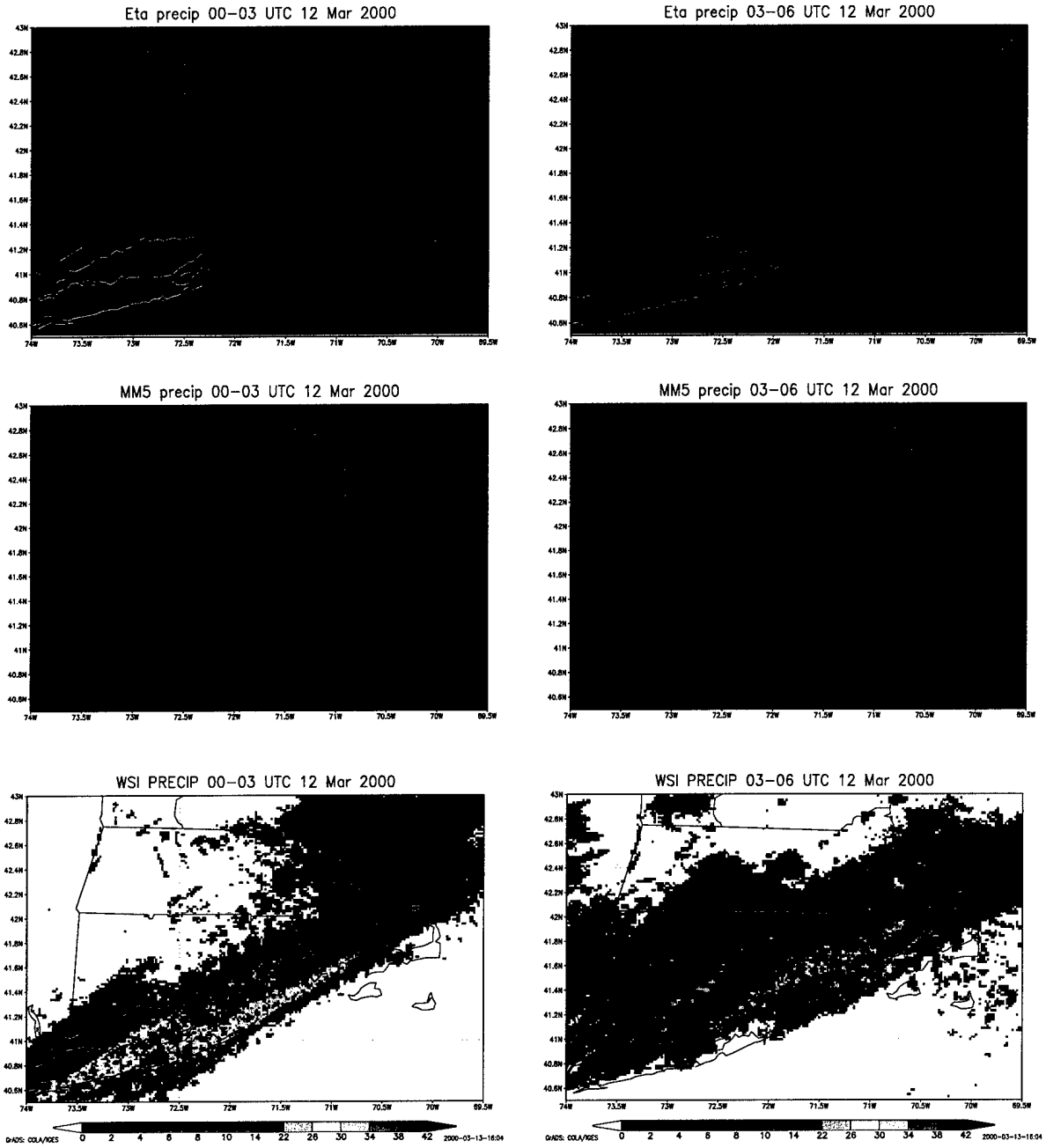

Figure 4: Precipitation forecasts and observations for 12 March 2000 over Southern New England. Shown are the Eta model (top row) and MM5 model (middle row) forecasts from 00 UTC, and verifying WSI PRECIP (bottom row) 3 hour accumulations (mm) ending at 03 UTC (left column) and 06 UTC (right column). Note the different levels of detail available from Eta, MM5 and PRECIP.

the holes from ground clutter subtraction and because of the overlap of radar sites, largely overcomes the effects of attenuation and range.

WSI's precipitation algorithms choose a specific rain rate (Z/R) for every NOWrad pixel (2×2 km) based on a unique empirical model developed and refined over a 6 year period. This model uses surface and atmospheric weather conditions in each 2×2 km pixel recomputed each hour from both observations and short term model forecasts. This approach is important since, it is not uncommon for precipitation to vary in nature and even form across the region covered by a single radar during a heavy precipitation event (e.g., convective to stratiform and rain to sleet to snow). By using a weather condition based approach, PRECIP is able to recognize and even compensate in situations involving hail or bright bands.

As a final step, each day, WSI meteorologists compare PRECIP output to official rain gauge observations and have the ability to apply a correction field to adjust for any biases or other factors that contribute to errors in estimates. WSI's PRECIP product is the best real-time operational blend of radar and other precipitation data available today.

During the first two years of operation (1991/1992) TASC compared PRECIP to rain gauge. That study found that 6 hour differences were less than 0.25 inches in 85% of all cases in which precipitation occurred and less than 0.50 inches in 92% of such cases. The mean departures were less than 20% for significant events (over .50 inches). Significantly, for rainfall in excess of one inch, the difference was less than 0.50 inches inch in 85% of the cases, and less than 0.25 inches in 65% of cases.

The PRECIP data have also been validated by Vollrath (1996 [49]). Vollrath analyzed the accuracy of PRECIP for an entire year (1 May 1994 thru 30 April 1995) over the CONUS by comparing PRECIP to the National Climate Data Center archive of hourly precipitation gauge records. Over 750,000 point comparisons were included in this study from 2,528 individual gauges. Vollrath showed that PRECIP at that time was most reliable in the Eastern and Central time zones. In the Mountain and Western time zones, topography and delayed installation of NEXRAD units results in an underestimation of the precipitation. Improvements were seen as the algorithm was updated.

3.2 Precipitation Forecasting Approaches

In principle, the NWP model precipitation should be ideal in all situations: NWP data assimilation can make use of all available data, and NWP models include the most complete description of the dynamics and physics of the atmosphere. In practice, a solution based solely on NWP modeling is risky, due to the loss of information in converting moisture parameters to the NWP model parameters, the problem of spin-up (Nehrkorn *et al.* 1993 [33]), and the inadequate methods of representing and assimilating moisture (Sundqvist 1978 [46]). Different techniques are superior at different time ranges and in different meteorological situations. To a certain extent, which techniques are superior at a given time range in a given situation is determined by the tradeoff between the sophistication of the physical processes represented by the technique and the loss of information when converting observations to the parameters needed by the technique. Thus at the very short range (approximately 0-6

h), extrapolation of radar precipitation imagery using correlation techniques is expected to be superior. The problems of the coarse resolution of NWP models and initialization of the precipitation in NWP models are demonstrated in the comparisons shown in Fig. 4. At longer ranges, depending on location and situation, NWP-based forecasts may be superior. At very long range, the best estimate may be climatology. (See Fig. 3.)

3.2.1 Advanced tracking algorithm for short-term precipitation

M.I.T. Lincoln Lab research has shown that convective storms in the CONUS can be broadly categorized into "air mass" and "line" storms. Air mass storms are small scale, seemingly random, fairly unorganized convective elements. Line storms are a collection of cells much like air mass cells, but they are maintained in a linear pattern, or "envelope." (See Fig. 5a.) Line storms maintain this pattern because they are typically forced at a large scale by a frontal discontinuity. In the summer months, the percentage of line storms is large in the north, while air mass storms dominate in the south. Line storms tend to dominate everywhere during the spring, fall, and winter months.

To determine line storm motion correctly, the large scale "envelope" motion must be found separately from the storm "cell" motion. Conventionally, people have forecast storms by extrapolating the motion of individual cells. For very short term predictions the cell motion is accurate, but for longer term predictions, the envelope must be tracked. The large scale (or envelope) motion is actually indicating the movement of the forcing mechanism for the convection, not the convective elements themselves. By separating the scales in the original weather radar image and tracking the large scale and small scale components separately, the motions of the envelope (large scale) and cells (small scale) can be found. In Fig. 5b, the large scale signal is moving southeast at 34 knots, while the small scale signal is moving northeast at 21 knots. The aviation weather group at M.I.T. Lincoln Lab has tested the new forecast technique on hundreds of hours of weather radar data. The Growth and Decay Tracker performs 52% better than the conventional cell tracker on line storms (Wolfson *et al.* 1999 [52]). Demonstration projects are currently continuing at four major U.S. airports.

3.2.2 Eta model

At longer forecast times beyond 3 hours we will use NWP model forecasts of precipitation from the Eta model, run operationally by NCEP at 00 and 12 UTC. An example precipitation forecast is depicted in Fig. 4. Currently, the Eta model, provides the best numerical guidance for precipitation forecasts over the U.S. While Eta is far from perfect, it is a considerable improvement over NGM (Mesinger 1996 [30]).

Eta includes all relevant dynamical and physical process (Janjić 1990, Zhao *et al.* 1997, and references therein [24, 55]). Convective precipitation is modeled using the Betts-Miller (1986 [5, 6]) convective adjustment scheme. The scheme was modified by Janjić (1994 [25]) to make it suitable for the extratropics. Nonconvective clouds are modeled using an explicit prediction of cloud water/ice mixing ratio (Zhao *et al.* 1997 [55]). The phase of the cloud

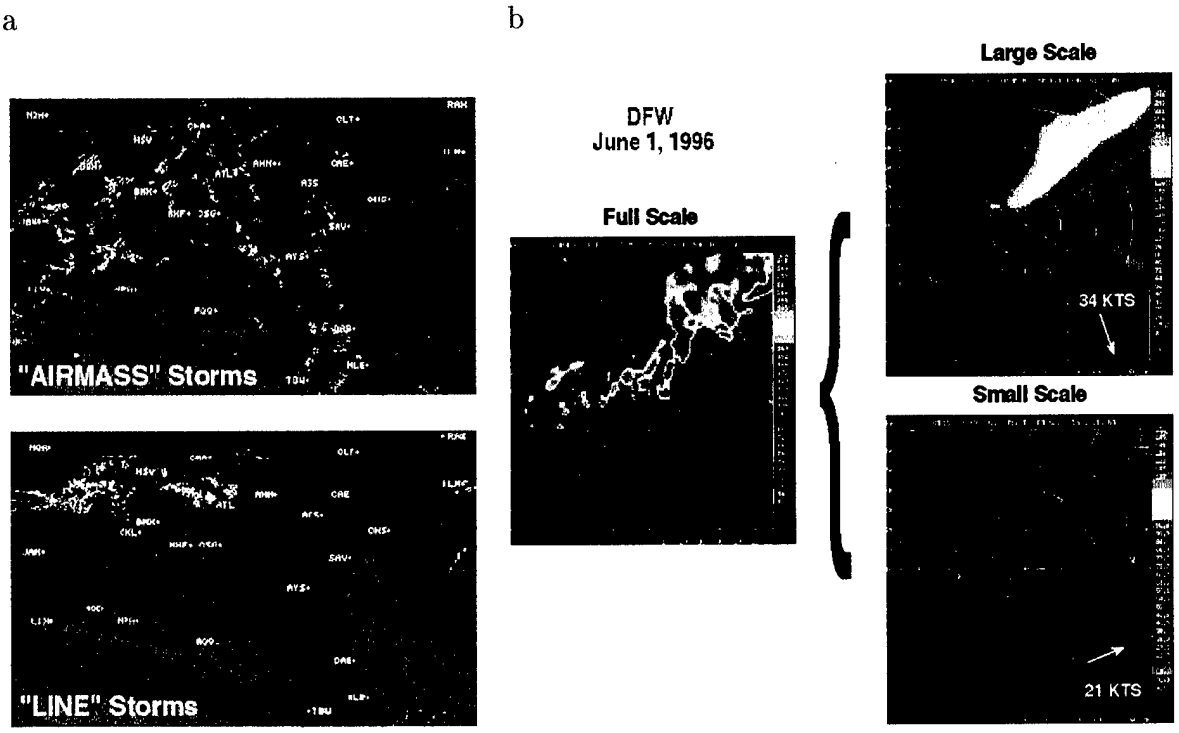

Figure 5: Short term precipitation forecasting. Typical cases of air mass and line storms are shown on the left (a). The separation of scales used by the "Growth and Decay Tracker" for the case of 1 June 1996 is shown on the right (b). The motion of line storms is better characterized by correlating the filtered or large scale images.

water and the precipitation rate are diagnosed from the predicted temperature and cloud water/ice mixing ratio in the column. Operationally, the cloud water is initialized from the first guess forecast.

At all forecast times, and for hindcasting tests, the Eta model will also provide the required fields other than precipitation, such as air temperature and humidity near the surface which are needed to parameterize evaporation. AER has developed various tools for real-time acquistion, decoding, and visualization of the Eta data. These tools were developed for an internal project to use Eta data as initial and boundary conditions for mesoscale atmospheric forecasts using the MM5 model.

3.3 Forecast Blending

To effectively use the different forecasts within R^2FS, a method of forecast synthesis is required. One approach is to choose one of the specific forecasts for each forecast time. A possibly more effective alternative is to blend the individual forecasts. The blending should be a Bayesian combination of the various forecasts. However, various approximations concerning the relevant statistics lead to different approaches.

Initially we will use the decision tree and accuracy adding techniques. In accuracy adding the blending weights are defined in terms of *a priori* information. Each specific forecast must have an accuracy, defined as the inverse of the error variance. Then, assuming uncorrelated errors between the specific forecasts, it is easy to calculate the blending weights. Further, the accuracy of the result is the sum of the accuracies of the specific forecasts. Accuracies vary with synoptic situation. A running estimate may be obtained by using persistence to forecast accuracy. For example, we could estimate errors of a 3 hour extrapolation forecast by comparing the current PRECIP field with a forecast initialized from the PRECIP fields of 3 hours ago.

3.4 Downscaling

Downscaling is important because the ratio between runoff and infiltration depends non-linearly on rainrate. Therefore a forecast only accurate in term of space time averaged quantities is not sufficient. While scales of precipitation observed by the current generation of weather radars ($\sim 2\ km$) are fine enough for the hydrology model, the NWP precipitation fields should be downscaled. The current operational grid spacing for Eta is 32 km. A purely stochastic approach was developed by Gong *et al.* (1994 [17]), in which the fractional area of each grid cell covered by precipitation is estimated from hourly precipitation records of individual observing stations. This method can be applied separately for each month of the year and thus indirectly takes into account the different statistical properties of stratiform and convective precipitation events prevalent during different seasons.

This approach can be extended by considering hybrid stochastic-dynamic and dynamic approaches to downscaling. Perica and Foufoula-Georgiou (1996 [38]) proposed a scheme in which the relationship between the scaling parameters and the amount of convective precipi-

tation is explicitly modeled based on the convective instability of the prestorm environment. The scheme was applied to mesoscale model simulations with resolutions of 36 and 12 *km* by Zhang and Foufoula-Georgiou (1997 [54]).

A conceptually simpler approach to downscaling is purely dynamical: to run a mesoscale model with a finer grid over the watershed. The benefit of higher resolution for mesoscale precipitation forecasting was recently demonstrated by Colle *et al.* (1999 [10]) for the case of the Pacific Northwest. There are subtle technical issues, however, which need to be carefully considered in such high-resolution model integrations: the physical parameterizations routinely used at coarser resolutions may no longer be appropriate at the higher resolution; the partitioning between explicitly resolved and parameterized ("convective") precipitation is highly dependent on model resolution, resulting in potentially very different model spinup characteristics (e.g., Zhang and Foufoula-Georgiou [54]).

We routinely run the MM5 mesoscale model in real time over the New England area (with nested grids at 30 *km* and 10 *km* resolutions) using Eta model fields as initial and boundary conditions. These model runs serve as a testbed for software and algorithm development. An example from a recent forecast is shown in Fig. 4, which shows the large-scale Eta model forecasts (produced at a 32 *km* resolution), the corresponding MM5 model forecast, and the verifying precipitation from the WSI PRECIP product for a 3 and 6 hour forecast. At both forecast lead times, the model fields are smoother and less intense than the corresponding observations, less so for the MM5 than the Eta. In addition, there is evidence of a spin-up problem in both the Eta and MM5 model fields for the first 3 hours of the forecast. At 3–6 hours, the MM5 field more closely reproduces the observed pattern of precipitation, although there are some differences in the details. In applications of the MM5 for downscaling of NWP model QPF to the basin level, even higher resolution runs of the MM5 (closer to the resolution of the radar data) could be used. Mesoscale models in general, and the MM5 in particular, have been successfully used to add detail to large-scale NWP model output by a number of researchers, e.g. Yu *et al.* (1999 [53]), Chen *et al.* (2000 [8]). While this dynamical approach is computationally expensive, it is feasible and should be tested.

3.5 Hydrological Model

CASC2D is a physically-based, two-dimensional, distributed-parameter, time-dependent, unsteady, infiltration-excess hydrological model for simulating the hydrological response of a watershed subject to an input rainfall field. CASC2D solves the equations of conservation of mass and momentum to determine the timing and path of runoff in the watershed. More traditional approaches rely on more conceptualizations of runoff production. The physically-based approach is superior when the modeler is interested in runoff process details at small scales within the watershed. Physically-based hydrological models are also superior when trying to predict the behavior of ungauged watersheds where calibration data do not exist. Major components of the model include:

Overland Flow: Two-dimensional, St. Venant equation using explicit finite difference. Uniform or spatially-distributed roughness based on land cover.

Channel Flow: One-dimensional explicit diffusive wave or implicit dynamic wave. Stream channel network through links and nodes.

Infiltration: Green and Ampt with or without moisture redistribution. Soil hydraulic characteristics based on soil texture.

Rainfall: Uniform or Spatially Distributed in Space and Time. Rain gauge and Radar estimated rainfall and combinations. Thiessen polygon or Inverse Distance Square interpolation.

Continuous Simulation: Hydrometeorology data (WES, SAMSON or NOAA/NCDC). Evapotranspiration (Deardorff or Penman-Montieth). Soil Moisture Redistribution.

CASC2D is included in the suite of hydrological models supported by the Watershed Modeling System (WMS) developed by Jones and Nelson at Brigham Young University. WMS is a comprehensive software package for developing computer simulations of watersheds which provides an interface to the hydrological model. (See Table 1.) The WMS software package is used at many sites, including federal, state, private, and educational institutions. WMS can be used for visualizing and delineating sub-basins in a watershed; computing hydrological and geometric parameters for each sub-basin; defining hydrological parameters that cannot be automatically computed; running several hydrological models; viewing the results of these hydrological models; and importing and exporting Geographic Information System (GIS) data.

Table 1: The CASC2D required inputs and outputs.

Inputs	Outputs
Digital Elevation Model	Outlet Hydrograph
Watershed Mask	Interior stream Hydrograph
Roughness	Overland Discharge
Retention Depth	Channel Discharge
Storage Capacity	Overland flow Depth
Initial Depth	Infiltration Depth
Interception Coefficient	Soil Water Content
Conductivity	Infiltration Rate
Wetting Front Capillary Head	
Porosity	
Soil Water Content	
Pore Distribution Index	
Residual Saturation	
Links and Nodes	
Rainfall rate	

CASC2D does not include redistribution of water through the groundwater system. This and other processes, are included in the M.I.T. Parsons Model and should be included in the next generation of operational hydrological models. Because the present formulation of CASC2D is completely modular, it should be easy to add such new processes. For example, we will consider how the redistribution of groundwater over complex landscapes results in varying depth to the water table over terrain. The surface hydrological flux (evaporation and runoff) are in turn enhanced in convergent areas surrounding the dendritic drainage network. Coupled modeling of hydrological processes in the saturated and unsaturated zones yields the spatial patterns of depth to the water table. Near the dendritic drainage network, the water table is shallow and there is a net discharge of moisture from the groundwater to the unsaturated zone. Conversely, in uphill regions, the water table is deeper (below the surface) and there is a net recharge to the groundwater system.

Lateral redistribution of water in the saturated zone is computed using approximation similar to the approach of Tarboton *et al.* (1995 [47]). For efficiency, this approach mixes analytical and numerical solutions. For example, transmissivities are obtained from the depth integration of hydraulic conductivities. Assuming transmissivities decay exponentially with depth leads to a simple analytical result dependent on depth to the saturated zone.

In the future the M.I.T. Parsons Model will be enhanced with evapotranspiration, snow accumulation and melt and canopy interception computations based on simple physical models. Evapotranspiration can be calculated using a Penman-Monteith approach with different formulations for dry or wet conditions and vegetated or bare surfaces. Bare surface evaporation can be calculated using a threshold method along the lines of Entekhabi and Eagleson (1989 [12]). Aerodynamic and canopy resistance can be calculated using wind velocities and vegetation properties. Snow accumulation and melt can be calculated through mass and energy balance considerations as in Wigmosta *et al.* (1994 [50]) and Anderson (1968 [2]). The above formulation has been preliminarily tested in a single model cell or pixel, with arbitrary, but reasonable forcing and conditions (Ganguly *et al.* 1997 [15]).

3.6 Verification Approach

To verify precipitation forecasts, we take the NEXRAD-based PRECIP estimates as truth. These data will be sufficient to validate the precipitation forecasts and can be used in hindcast mode to drive the hydrological model. As a preliminary we will verify the accuracy of PRECIP versus gauge data. Of course further enhancement to PRECIP are possible, but for current work, PRECIP provides a uniform, complete data set which is continuous in space and time. In this context, hindcasts using only the PRECIP estimates can be used to validate the hydrology model alone.

Verification of the MIT distributed model is presently taking place with the support of NASA and the National Weather Service Office of Hydrology. The traditional performance criteria developed for lumped hydrological models (matching hydrographs at a single outlet) is not adequate for a spatially-varied system. The classical verification and forecast skill evaluation methodology used in weather forecasting is spatial but it lacks temporal dynamics

(Murphy and Winkler 1987, Charba and Klein 1980 [32, 7]). Furthermore, the amount of verification (observed) data is limited in the case of runoff generation and hydrological response. In future work the verification task will consist of both long-term water balance components and event-based (for both storm and interstorm events) hydrological response. Procedures for naturalized flow generation will be used for those river gauges that are downstream of hydraulic structures. Although necessary, this approach to verification is not rigorous enough to fully discriminate the performance of a distributed model. In this project we will also test the event response of the model in order to test components of the distributed system. For example, the categorical, event oriented, flood forecast verification and skill evaluation scheme of the National Weather Service will be used to verify components of the flood hydrograph at a river gauge location (Morris 1988 [31]). During the interstorms (following storm events that are well-captured), the rate of decline of the hydrograph recession limb is used to test the groundwater discharge component of the distributed model. The ensemble performance of the model over the river basins across a number of forecasted precipitation and temperature events will then be estimated. In addition, methods for quantifying the skill in reproducing the spatially-varied flood response will be developed. With appropriate validation data sets for extreme hydrologic events (i.e. floodplain indundation from satellite imagery), the distributed hydrologic model can be truly tested as a flood forecasting tool.

3.7 Satellite measurement of rainfall

Satellite-derived precipitation can replace radar estimates in our system, but initial R^2FS development will be based on NEXRAD. Research on space-based rain estimation has been continuing for several decades with a large number of methods appearing in the literature. Many of these methods use combinations of either visible, infrared, and passive microwave measurements applied in statistical, physical, or combined statistical-physical approaches. The results of several international algorithm intercomparison studies (e.g. Smith *et al.* 1998 [44]) have yielded little consensus on the optimum approach, with no method showing a consistently superior performance. However, one feature which emerges from these studies is that most methods exhibit some degree of "climatological bias". That is, each method performs better on the data to which it was tuned, than on other independent data sets. This is manifested in regional and seasonal biases, and is true not only for purely statistical methods, but also for physical methods which are based on cloud and hydrometeor models and on radiative transfer calculations which are biased implicitly due to various modeling assumptions.

Typical infrared-based algorithms are Arkin (1979 [3]); Arkin and Meisner (1987 [4]); and Janowiak (1992 [26]). Algorithms making use of passive microwave measurements include Wilheit and Chang (1980 [51]); Spencer (1986 [45]); Olson (1989 [35]); Kummerow *et al.* (1989 [27]); Grody (1991 [21]); Liu and Curry (1992 [29]); and Petty (1994 [39]). Adler *et al.* (1993 [1]) used a combination of infrared and microwave data, in fact using SSM/I data to recalibrate a simple IR scheme, while Ferraro and Marks (1995 [14]) used SSM/I data to calibrate a microwave emission and scattering algorithm against ground-based radar

rain rates. Recently, Grassotti *et al.* (1999 [20]) used SSM/I rain rates to tune a VIS-IR threshold method for application to heavy rain flagging of scatterometer wind data. In the context of numerical weather prediction Grassotti and Garand (1994 [18]), and Garand and Grassotti (1995 [16]) used a multifeature classification approach to combine visible and infrared imager data with rain rate fields from an operational forecast model. Researchers at AER continue to be actively engaged in novel ways to combine satellite and ground-based radar measurements (Grassotti *et al.* 1999 [19]).

The recently launched TRMM satellite (Simpson *et al.* 1988 [43]) addresses the need for more accurate rainfall measurements in the lower latitudes. The TRMM suite of instruments includes an active precipitation radar, passive microwave sensors, as well as visible and infrared imaging sensors. Recent work by Kummerow and collaborators (Olson and Kummerow 1996; Olson *et al.* 1996; Kummerow *et al.* 1996 [37, 36, 28]), has focused on combining the passive and active microwave measurements from TRMM to improve the characterization of the cloud and hydrometeor profile, and the surface rain rate. However, the TRMM orbit coverage is only in the region between roughly 35°N and 35°S.

For coverage in the midlatitudes, polar orbiting satellites such as the NOAA KLM series which contain both well-calibrated VIS, IR, and passive microwave sensors, or microwave data from the DMSP SSM/I sensor are available. The newer geostationary meteorological satellites also have useful VIS and IR channels for rainfall estimation, and full disk coverage every 30 minutes or better. Because the VIS-IR methods of rainfall retrieval are less direct than microwave-based algorithms, it is critical that they be frequently retuned to remove, to the extent possible, the regional and seasonal biases which are likely to occur. In the case of microwave data, the most serious limitation is the lack of sensitivity over higher emissivity land surfaces.

3.8 Ensemble forecasting

Currently we focus on the deterministic forecast. In general, however, meteorological forecasts, and precipitation forecasts in particular, are probabilistic in nature. In later phases of this project, R^2FS could be used to produce probabilisitic QPF and probabilistic flood forecasts based on NCEP's ensemble NWP products. Although computationally expensive, the ensemble forecast technique is appropriate because both the NWP and hydrology models are very nonlinear. The ensemble forecast method is now useful in NWP at long range. It is noted that the pool of potential forecasts increases dramatically if somewhat older forecasts verifying at the correct time are included in the ensemble (Hoffman and Kalnay 1983 [22]). Currently ensembles of NWP model runs are available operationally. Thus probabalistic forecasts may be simply based on the NWP ensemble and an associated ensemble of runs of the hydrological model.

4 Phase I Accomplishments

The Phase I effort resulted in the development, testing and application of a prototype R^2FS for hydrometerological modeling. In this prototype, pre-existing system components were used in conjunction to model the watershed response to a rainfall event obtained from the WSI value-added NEXRAD product. The baseline hydrologic model WMS-CASC2D was implemented with a realistic channel geometry, soil moisture distribution, and channel network. Distributed rainfall inputs from the actual 2 $km \times 15$ min WSI rainfall data were used to produce a model runoff response which was compared to a U.S.G.S. streamflow observation at the watershed outlet. A series of sensitivity studies performed during the calibration and validation series revealed the model sensivities to particular parameters. This exercise constitutes substantial progress in integrating, testing and applying the R^2FS prototype.

The specific technical goals which have been accomplished during Phase I to implement the R^2FS prototype are:

1. Set up a ground station to receive WSI data products.
2. Acquire NCDC gauge data.
3. Capture and archive Eta forecasts.
4. Capture and archive WSI PRECIP fields.
5. Acquire USGS streamflow data.
6. Develop software to decode gauge, forecast and radar data.
7. Validate PRECIP data against gauge data.
8. Obtain and implement the CASC2D and WMS.
9. Obtain model data (DEM, soils, landuse) for watershed application.
10. Analyze data using Geographical Information System (GIS).
11. Model calibration and sensitivity exercises.
12. Application of prototype to synthetic and WSI PRECIP rainfall data in selected test watershed.

These accomplishments are described in more detail in § 4.2 and § 4.3.

4.1 Data Acquistion

For model testing and validation, three sources of precipitation data were obtained during the reporting period: rain gauge measurements from NCDC, gridded radar data from WSI (based on original NEXRAD scans), and Eta forecasts from NCEP.

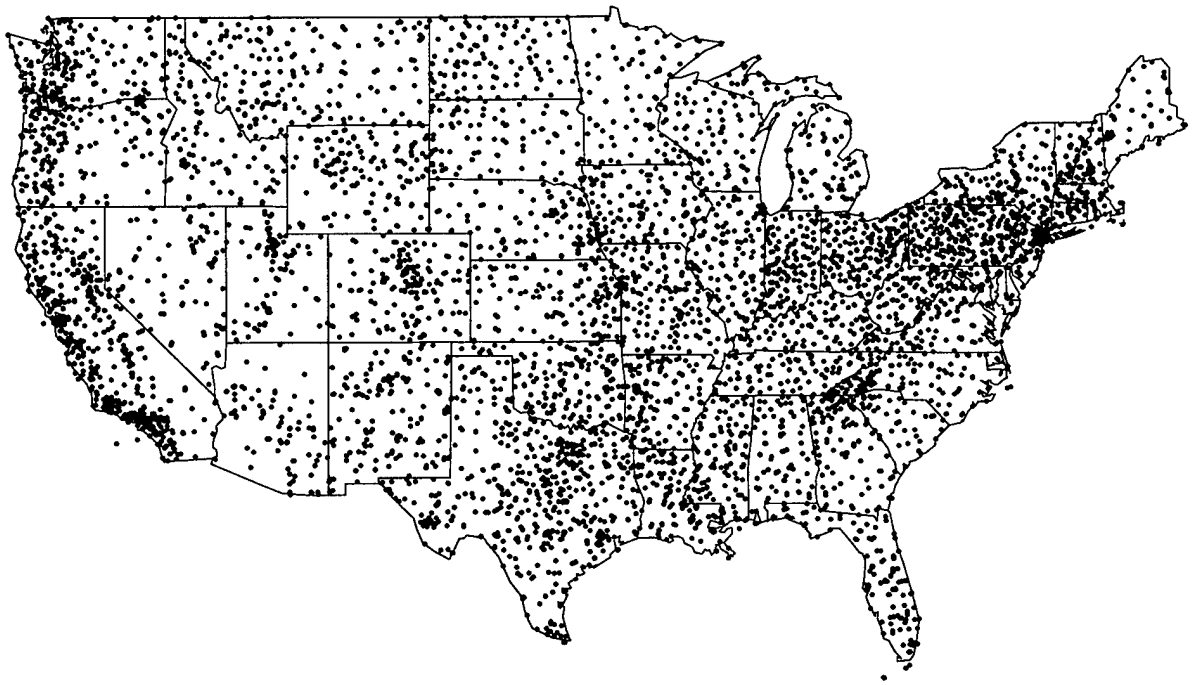

Figure 6: NCDC rain gauges present in the data base for the CONUS.

4.1.1 NCDC rain gauge data

The first precipitation data we have obtained are the hourly surface rain gauge observations for the entire U.S. Fig. 6 shows the coverage available from this dataset. The dataset was obtained from Hydrosphere, Inc. through an existing purchasing arrangement between Hydrosphere and MIT, and involved no additional expenditure. The data are the same as those available publicly from NCDC, but in a more readable format. These data cover the period from 1948 through September 1998. We have also developed software to reformat, and visualize these data to facilitate validation of the WSI precipitation data.

4.1.2 WSI PRECIP

Under agreement with WSI we purchased and installed a WSI data ground station on site at AER. Under this agreement, WSI provides access to the data stream at no cost, for the duration of the project. The advantage of using the WSI product is that the data have already been quality controlled, reducing and removing known radar artifacts such as range fading and ground clutter. Examples of the WSI data are shown in Fig. 4, and in Fig. 8, discussed below.

Considerable effort was required to create new codes and to modify existing decoding software to ensure regular reliable archiving of the data. These data are broadcast every 15 minutes, and since mid-December we have received data nearly continuously. M.I.T. Lincoln

Lab provided us with software for archiving and decoding the WSI data and with copies of the WSI data that they had archived previously. We modified the decoding and archiving software for our use. We also have developed codes to visualize the rainfall data, based on user-specified time and location selection criteria. These are necessary to aid in case selection. We also have developed software to convert the archived 15-minute and hourly data to formats suitable for input to CASC2D.

The WSI NEXRAD precipitation data are available in several forms. For our work the most appropriate version is called "SPECIAL", while the name "PRECIP" is reserved for another version, the accumulated total precipitation. In this document we use the term PRECIP to refer to all these data generically or to the SPECIAL data specifically. The PRECIP data are gridded, covering the CONUS. Because so many values are zero, PRECIP is run length encoded. The grid is 2 km N-S by ~ 1.7 km E-W (depending on latitude) by 15 minutes. The reported values are valid for the interiors of the grid cells defined by the following grid parameters:

	start	end	number
latitude	53N	20N	1838
longitude	130W	60W	3662

where number is the number of grid cells. For SPECIAL, the rainfall is quantized in units of 0.05 inches/15 minutes, so values of 0, 1, 2, 3 correspond to rainfall of 0, 0.05, 0.10, 0.15 inches for the 15 minutes ending at the reported time. To convert the integers values to mm/hr, multiply by 5.08. Note that SPECIAL includes only rain—snowfall amounts are set to zero.

We began archiving WSI PRECIP and SPECIAL data since mid October 1999. Appendix A contains an inventory of what we have for SPECIAL data. For each calendar day we list the number of files per day. A complete day would have a count of 96. Overall the holdings are spotty. Since 19 December 1999 we have been doing very well at collecting these data at AER. Before October we have filled in with the archived data from M.I.T. Lincoln Lab.

4.1.3 Eta model output

The Eta model output has been captured and archived in real-time at AER, starting in August 1999. A near-complete archive of GRIB files has been accumulated, consisting of 00 UTC and 12 UTC forecast fields out to 48 hours, at 3 hours intervals. All model fields are available on a 40 km grid, at a variety of vertical levels, including the surface, near-surface (shelter and anemometer level heights), and pressure levels (every 25 hPa).

There are a number of fields directly applicable to QPF and downscaling: accumulated precipitation (stratiform and convective), precipitation type (rain, snow, ice pellets), and convective indices (CAPE, lifted index). Others are of relevance for the surface energy and water budget calculations (near-surface winds, humidity, and temperature, surface radiative and turbulent fluxes).

4.2 Precipitation Depiction and Validation

In order to verify the accuracy and observational characteristics of the WSI SPECIAL data we conducted a limited validation study by comparing these data with surface rain gauge observations in the 4-state region (Oklahoma, Arkansas, Missouri, and Kansas) surrounding one of our case study river basins, the Baron Fork. The locations of the gauge and radar sites are shown in Fig. 7. We performed validation for several storms which occurred during January and March of 1998, and looked at validation results for each of these four states. In particular, we identified three precipitation events occurring on 3–8 January, 7–8 March, and 15–20 March. The time series of WSI SPECIAL maps for 4 January, shows the motion and development of a frontal rain band across the region (Fig. 8).

We validated the WSI radar estimates by comparing against gauges for both accumulated rainfall and instantaneous rain rates. We first consider storm total accumulations for the three selected precipitation events. Fig. 9 shows scatterplots of radar versus gauge total accumulated rainfall during the 6-day 3–8 January event broken down by state. Each point in the plot is a radar-gauge collocation. In all states, the agreeement between radar and gauge observations is good, albeit with a tendency for the radar to slightly underestimate rainfall with respect to the gauges.

Fig. 10 and Fig. 11 show results for the remaining storm events. Results are similar to those for the 03–08 January event, indicating a tendency for radar underestimation with respect to gauges and correlation coefficients in the range 0.3–0.9 depending on the state and storm event.

Fig. 12 shows the spatial distribution of the radar-gauge differences overlaid on a map of the total radar accumulation during the storm. We note the largest differences are associated with areas of heaviest rainfall, and the presence of a large positive outlier in Arkansas. Closer examination of the outlier revealed what was clearly a bad gauge which reported no rainfall during the entire period.

Fig. 13 and Fig. 14 show results for the 7–8 March and 15–20 March storms, respectively, using the same convention as in Fig. 12. Except for an area in southwest Arkansas where radar accumulations exceed those for gauges, the radar is generally seen to underestimate rainfall with respect to gauges. Both figures show clear artifacts of the radar processing, due perhaps to range fading and ground clutter. Note, for example, the circular patterns in the accumulation fields near (38N,90W), (37N,93W), (37N,98W), and (35N,102W). Also note the erroneously high values in Kansas near (39N,95W), probably due to ground clutter. These indicate that the WSI data need to used with care in certain regions. Also interesting are the small scale wave-like patterns which are evident in all three accumulation images. The fact that they occur in slightly different areas in each storm makes it less likely that they are radar-site artifacts. However, they may possibly indicate terrain or storm-induced mesoscale waves.

For forcing the hydrological model, it is important to have credible rainfall estimates for shorter timescales. Therefore we also examined results for near-instantaneous rainfall estimates. Fig. 15 shows a number of time series for the 6-day period 3–8 January at gauge sites over Oklahoma. It is encouraging that even at this time scale the radar (black curves)

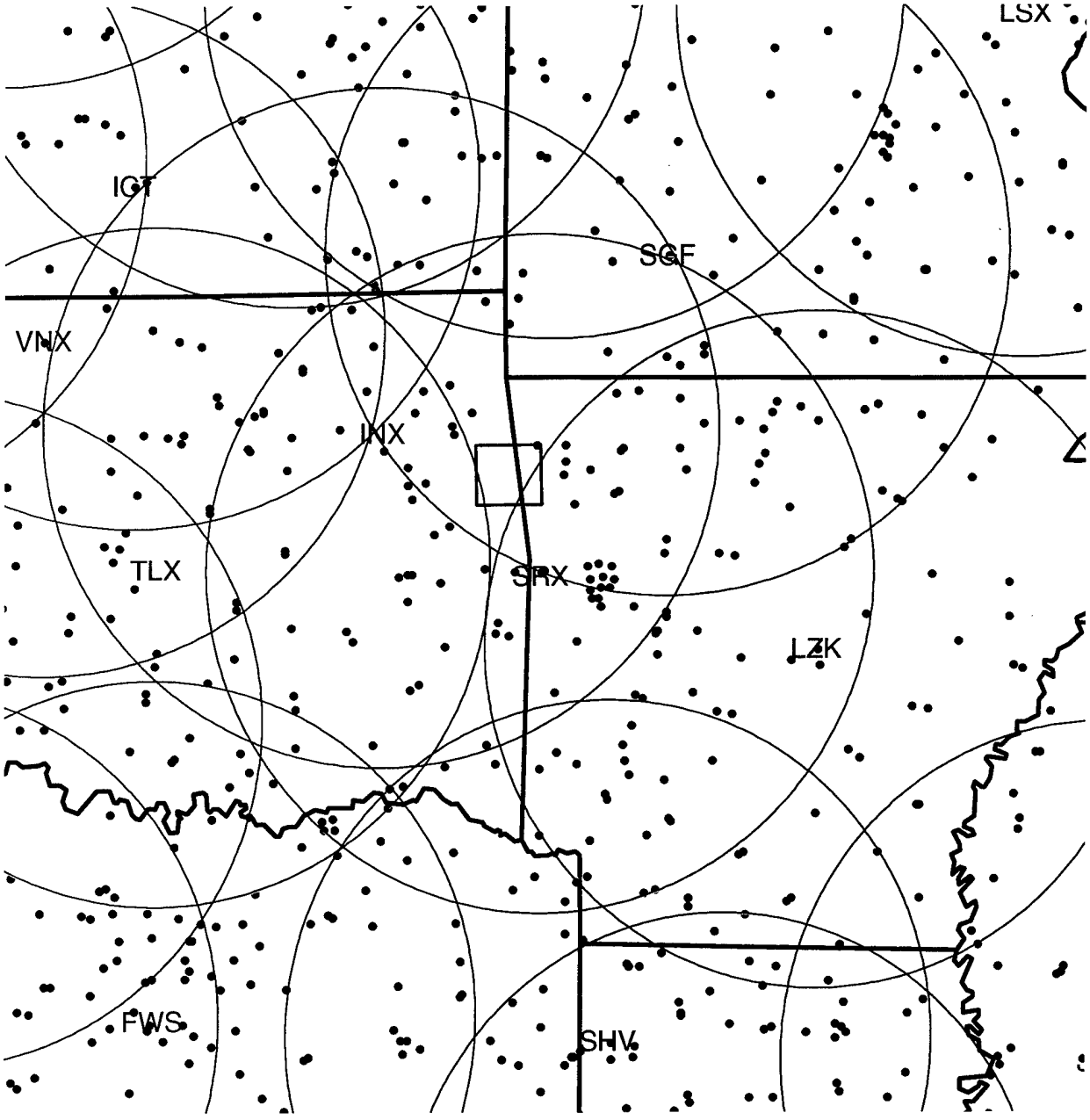

Figure 7: Data coverage centered on Baron Fork. Gauge locations are in red. NEXRAD locations and nominal coverage are in green.

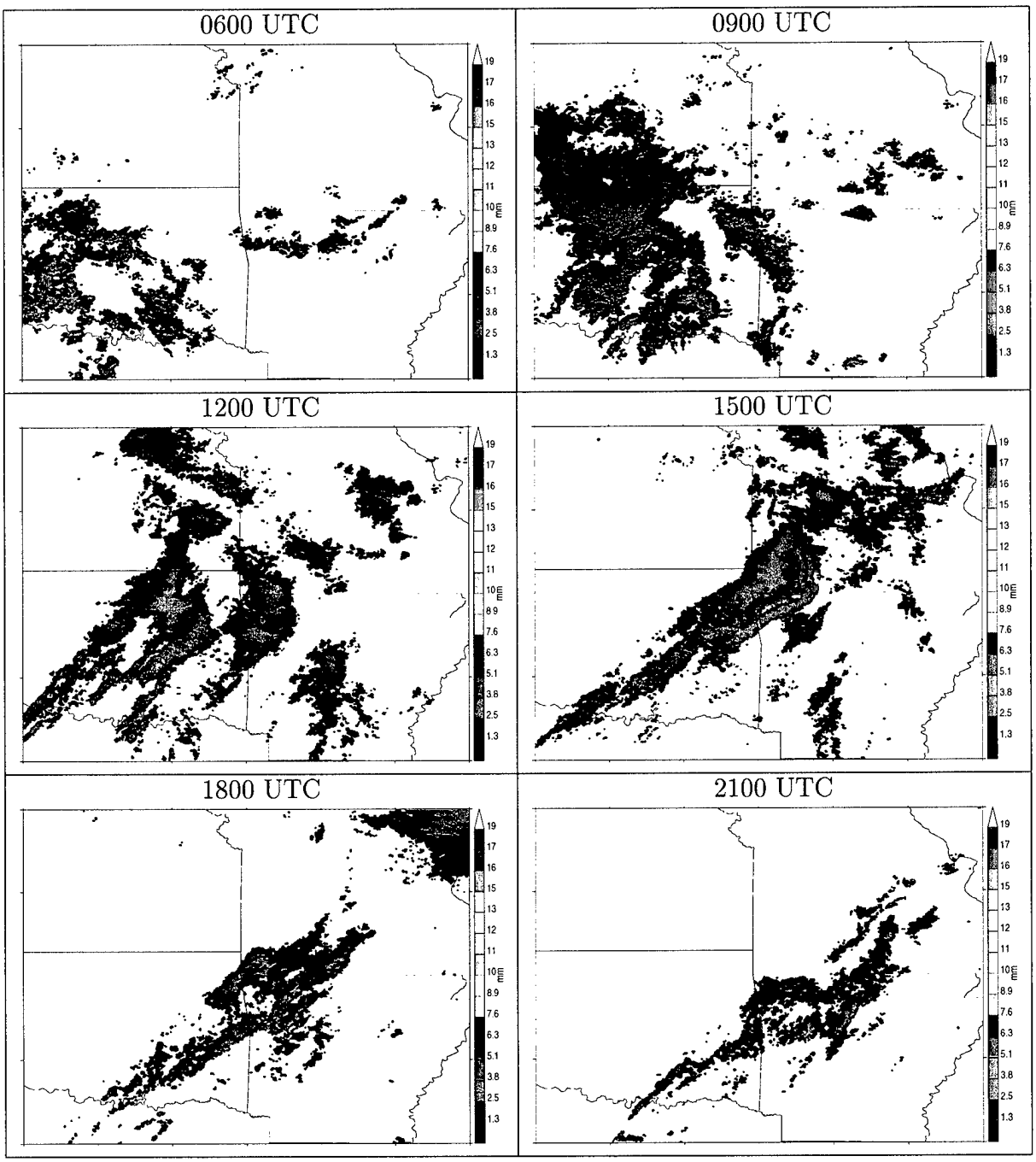

Figure 8: The PRECIP time series for 4 Jan 98, in mm per 15 minutes. The individual images are separated by 3 hours. Note the overall eastward drift.

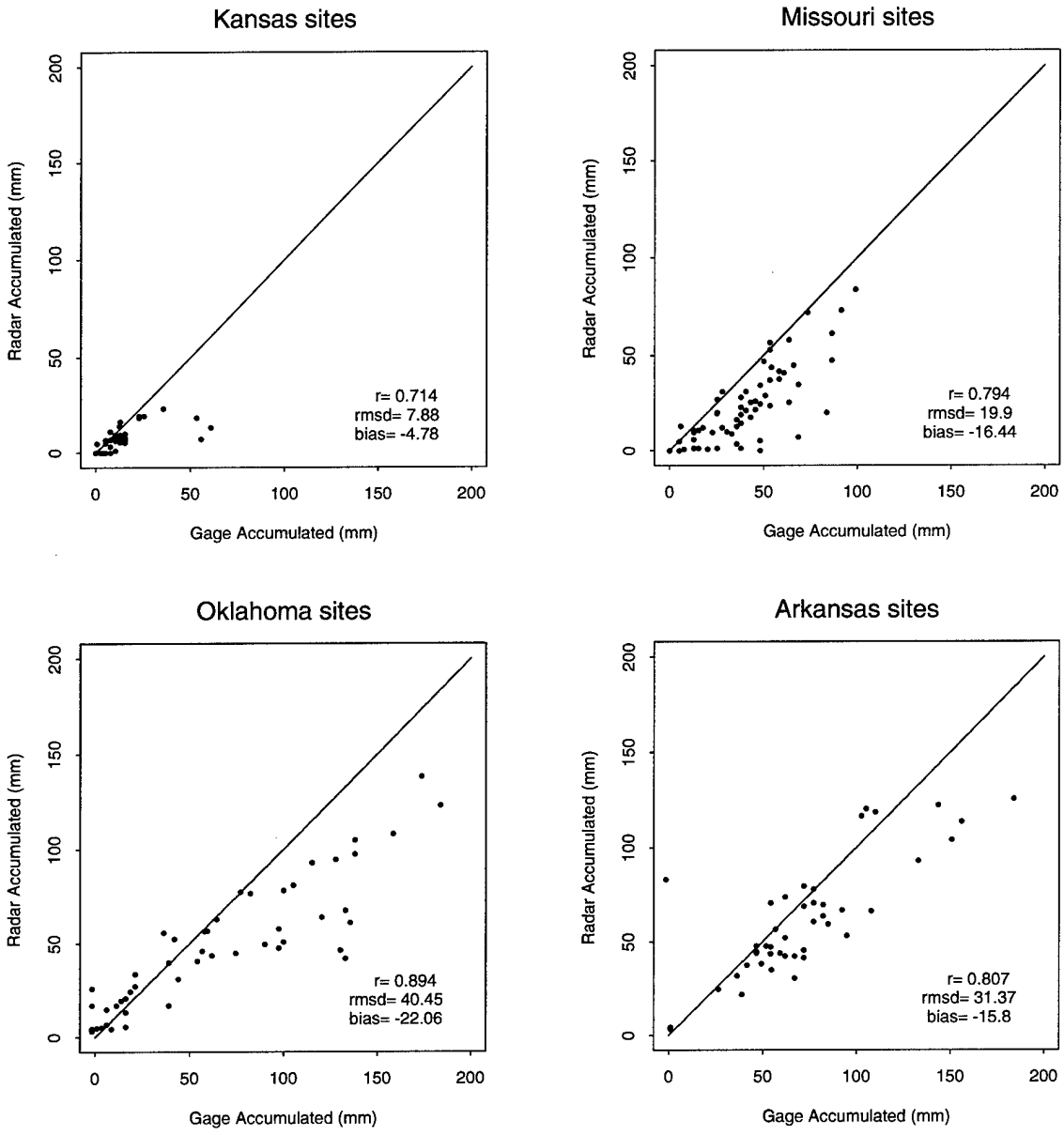

Figure 9: Radar versus rain gauge scatterplots for the storm of 3–8 January 1998. There is generally good agreement between these two estimates of precipitation.

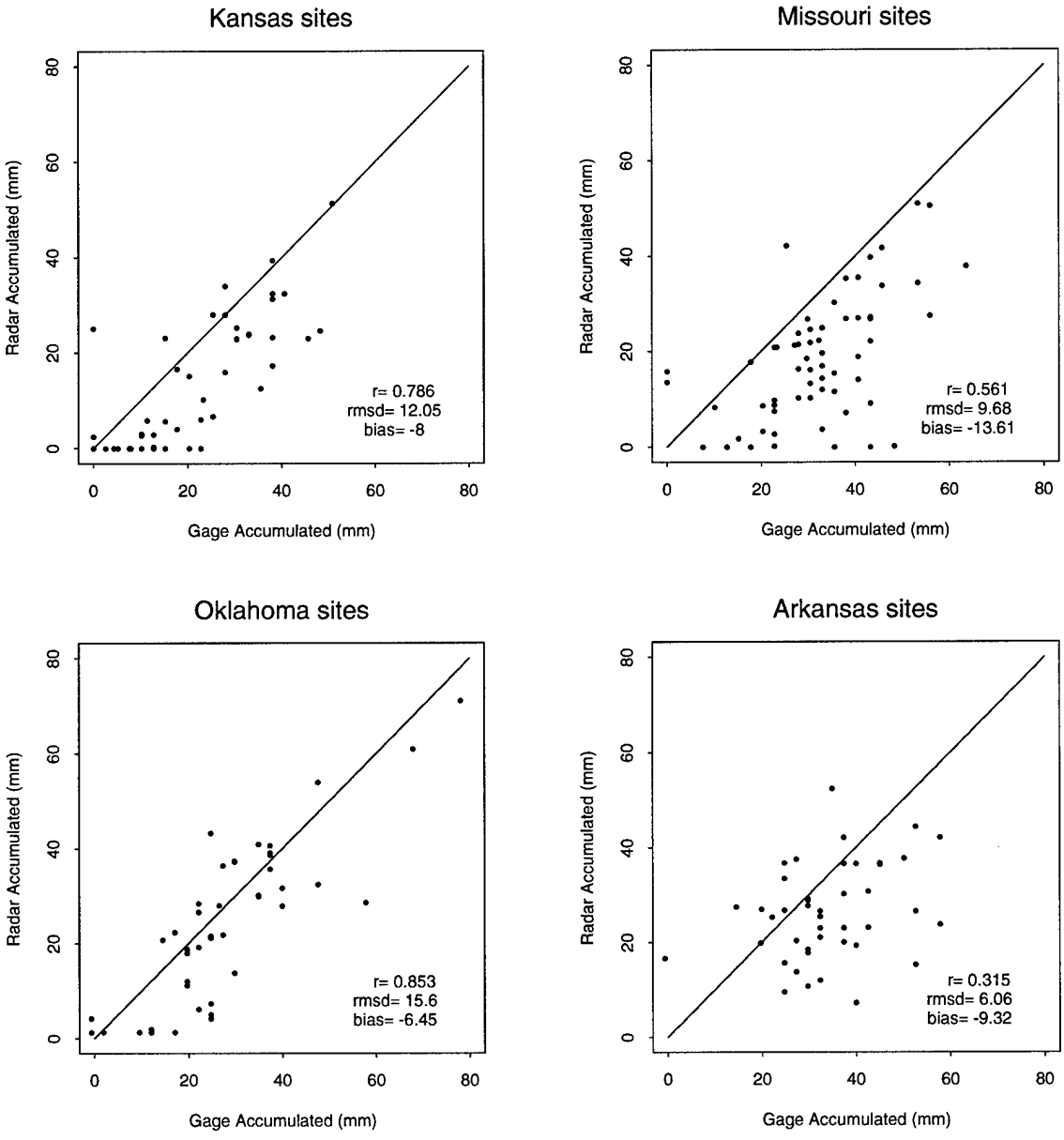

Figure 10: Radar versus rain gauge scatterplots for the storm of 7–8 March 1998.

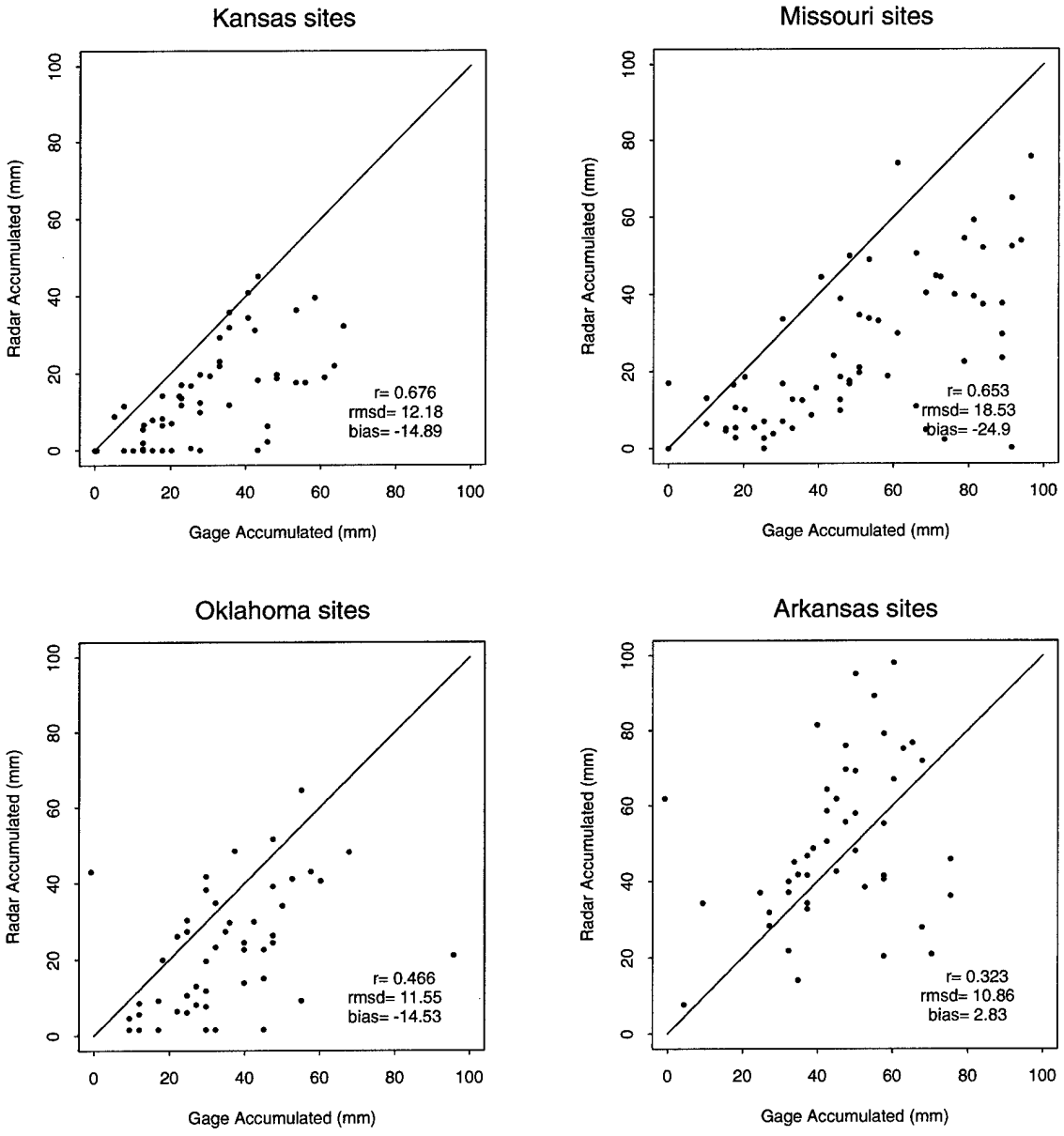

Figure 11: Radar versus rain gauge scatterplots for the storm of 15–20 March 1998.

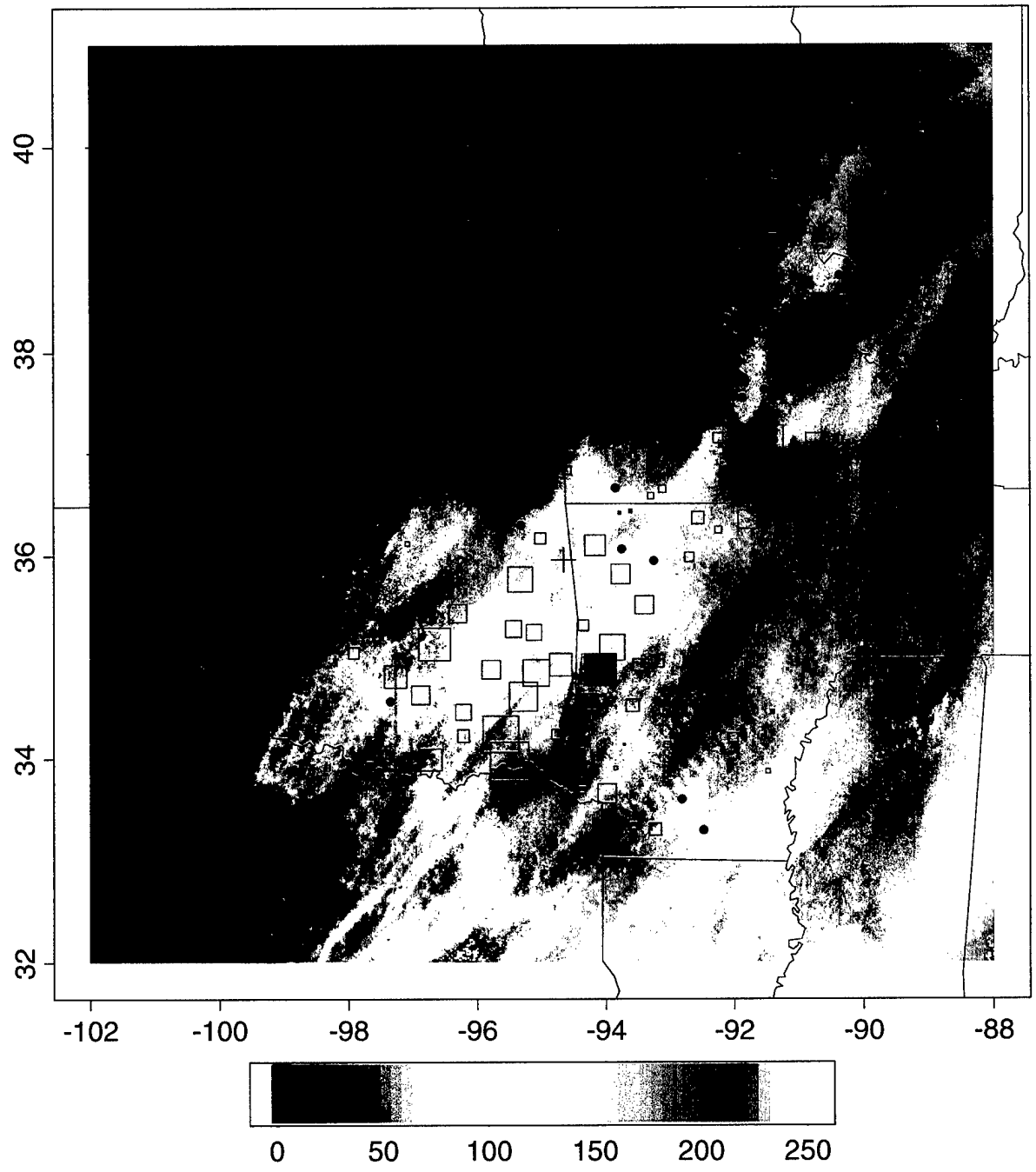

Figure 12: Gauge and radar map intercomparison for the storm of 3–8 January 1998. The image shows the radar estimated storm total in mm. Red squares are sized proportionally to the difference between the estimates of storm total precipitation. Filled red squares indicate that the radar estimate is larger. Filled black circles indicate that the differences were within ± 5 *mm*.

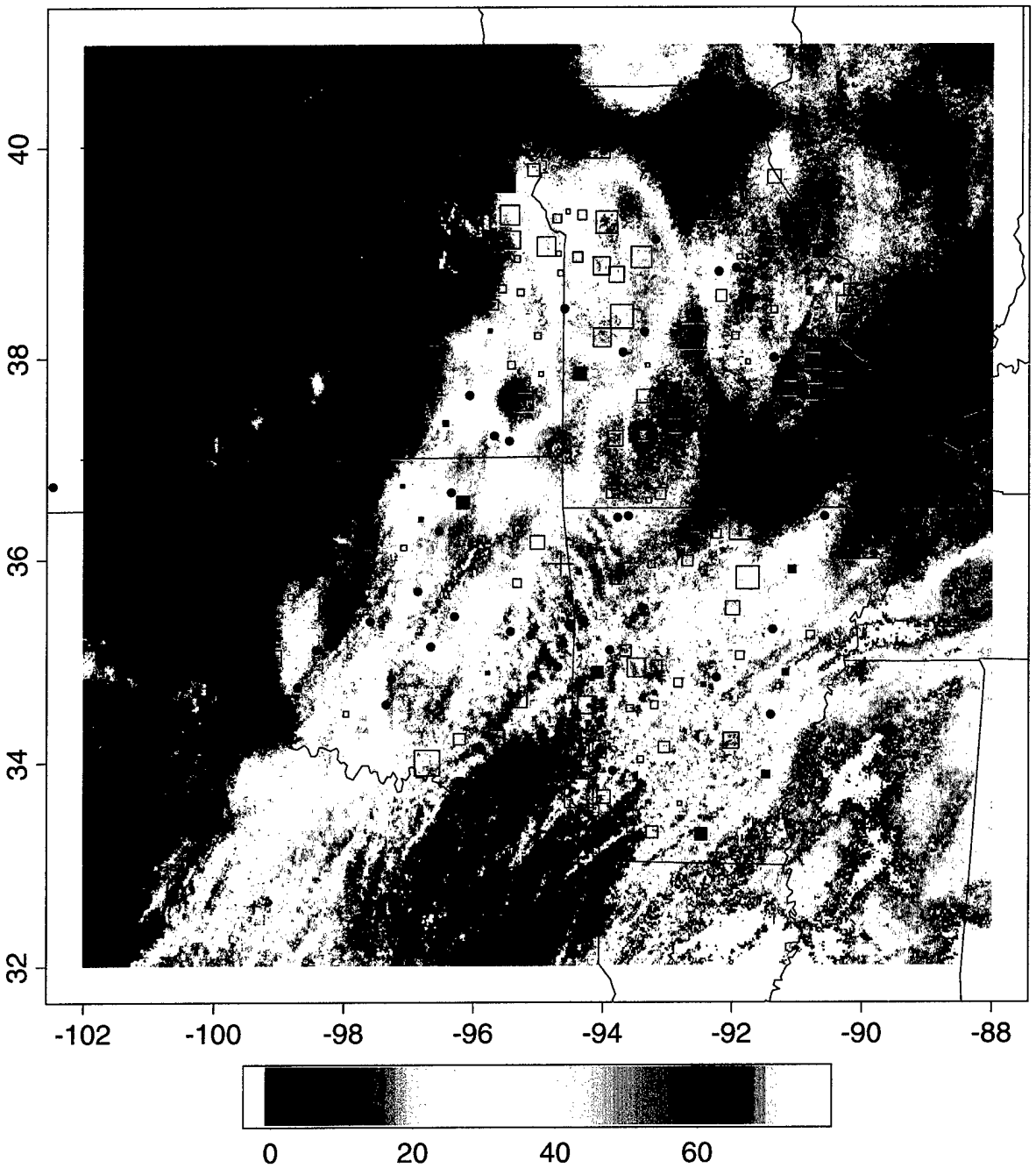

Figure 13: Gauge and radar map intercomparison for the storm of 7–8 March 1998. Plotting convention is same as in Fig. 12.

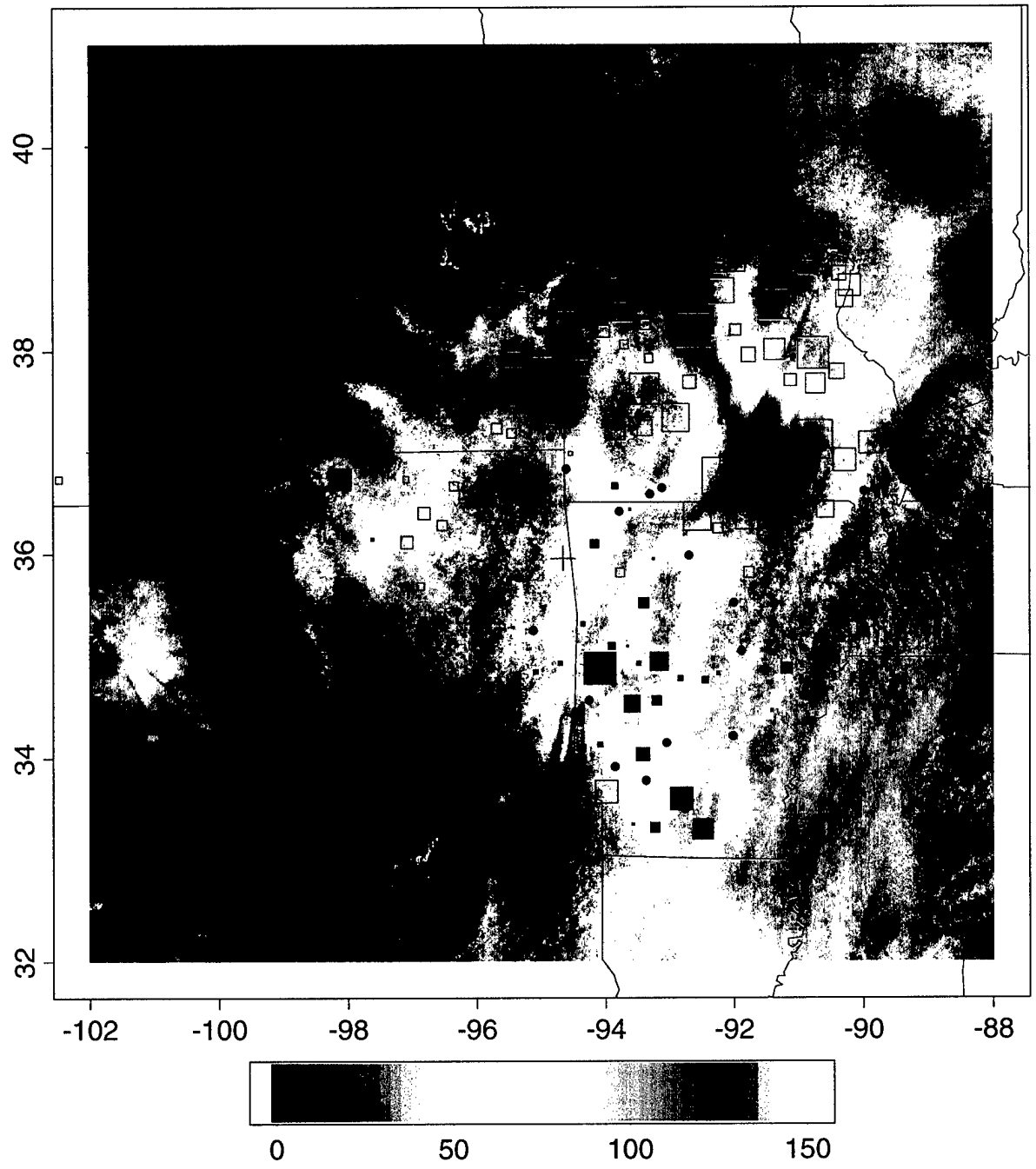

Figure 14: Gauge and radar map intercomparison for the storm of 15–20 March 1998. Plotting convention is same as in Fig. 12.

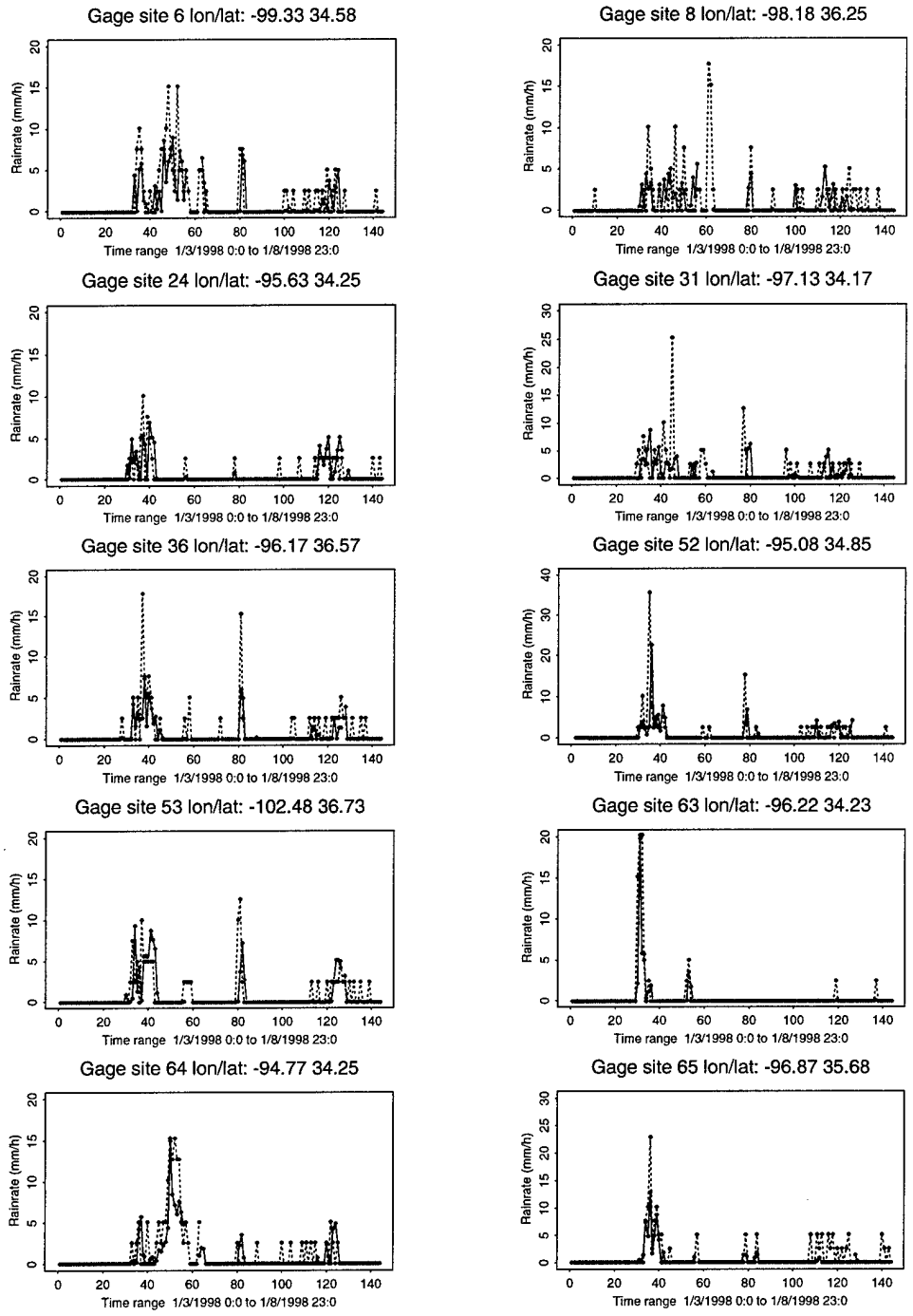

Figure 15: Gauge (red) and radar (black) time series are compared for the storm of 3–8 January 1998, at selected sites.

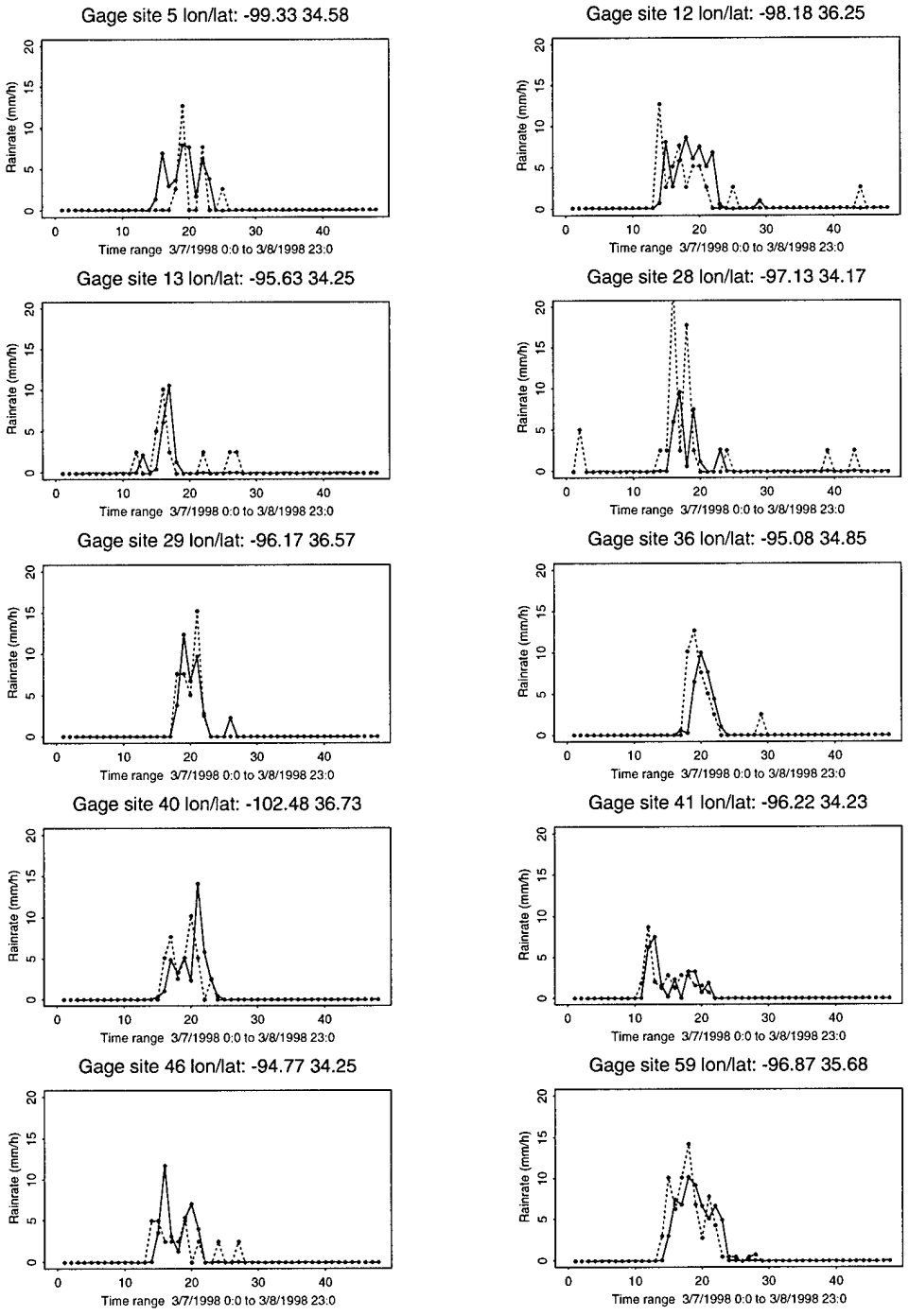

Figure 16: Gauge (red) and radar (black) time series are compared for the storm of 7–8 March 1998, at selected sites.

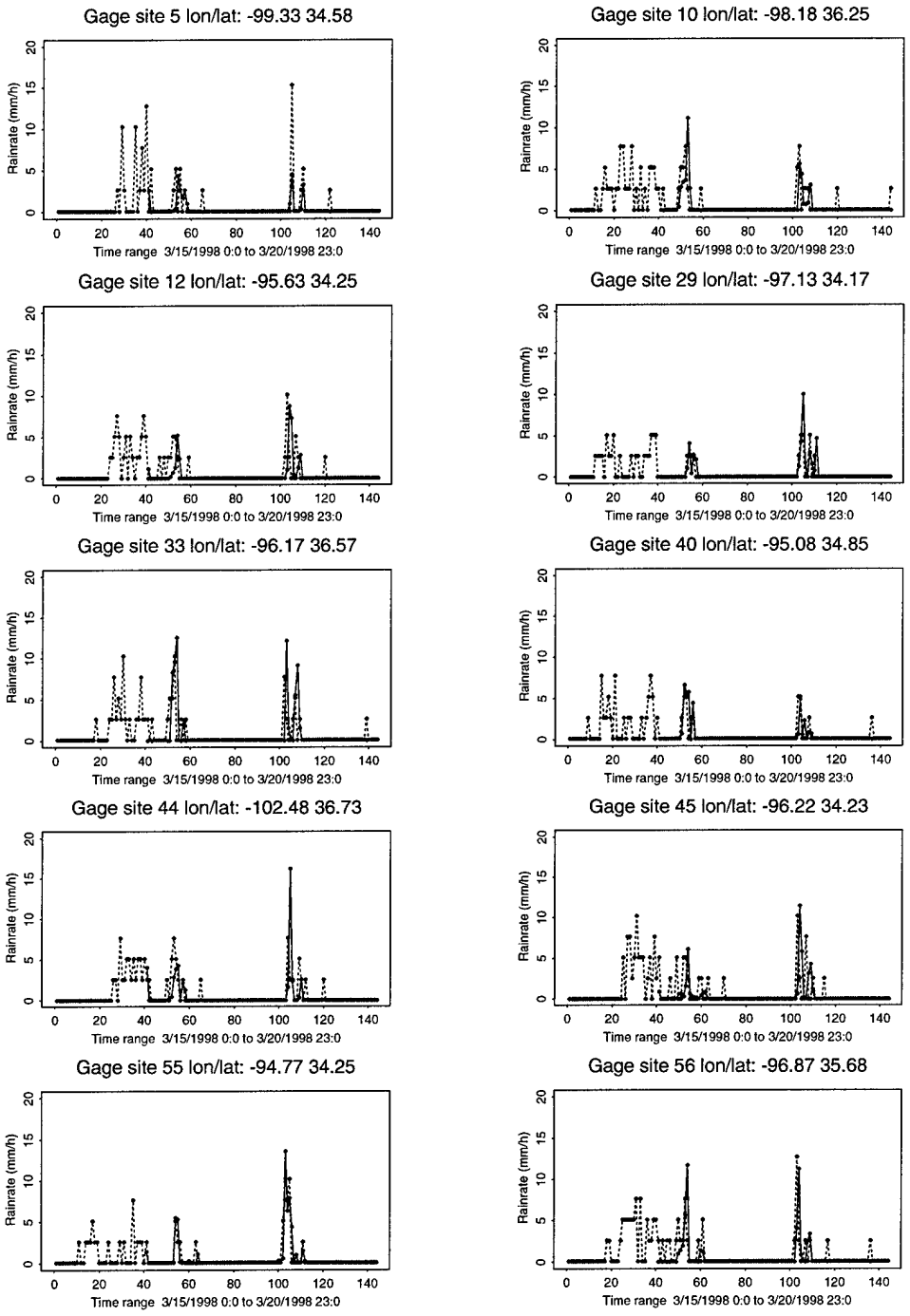

Figure 17: Gauge (red) and radar (black) time series are compared for the storm of 15–20 March 1998, at selected sites.

and gauges (red curves) are in extremely good agreement. However, as was the case for storm-accumulated rainfall, the general characteristic of the radar to underestimate peak rain intensity for individual rain events is also quite evident.

Similarly, Fig. 16 and Fig. 17 show results for selected Oklahoma gauges during 7–8 March and 15–20 March. Again we see fairly good agreement between radar and gauge. Nevertheless, there are notable exceptions. During 15–20 March, the initial 20-hour burst of rain recorded by most of the gauges is not observed by the radar at any of the gauge sites shown, despite the fact that the gauges were reporting rates in excess of 5 mm/hr.

Finally, Fig. 18 shows a jittered scatterplot of the radar vs. gauge instantaneous rainfall for the 3–8 January storm over all four states. Only modest agreement is seen at this time scale, with correlation coefficients below 0.5. Moreover if the "no rain" points are excluded from the plot the correlations generally drop below 0.2. Nevertheless, this is consistent with numerous other studies which have compared instantaneous rainfall measurements. The high spatio-temporal variability of precipitation, and the inherent sampling differences of the gauge and radar observing systems makes closer agreement unlikely. Also note the effect of the gauge reporting discretization of 0.1 in (2.54 mm/hr).

Table 2: Contingency table for 3–8 January 1998.

	Gauge-No Rain	Gauge-Rain
Radar-No Rain	4320	340
Radar-Rain	361	472

Table 2 contains a rain/no rain contingency table for the 3–8 January storm. If points in which both radar and gauge record no rain are excluded, then there is agreement between radar and gauge for raining points slightly over 40% of the time.

4.3 Hydrological Modeling

Significant progress was made in implementing the hydrological component of R^2FS. Due to the distributed nature of the model, CASC2D requires the user to characterize the topography and soil surface features of the watershed under study. In the preliminary application of R^2FS, four watersheds were chosen based upon considerations of data availability and heterogeneity in climatic and topographic factors. Two of these watersheds are located in the northeastern corner of Oklahoma (Baron Fork and Peacheater Creek basins, see Fig. 19), while the other two are located in the Appalachian region of northern West Virginia (Cheat River and Dry Fork basins, see Fig. 20). The latter basin in each pair is nested within the former basin, allowing for the investigation of spatially distributed radar rainfall over selected portions of the larger basin. Due to modeling efforts using the Sacramento Model and the M.I.T. Parsons Model on the Peacheater Creek basin, this watershed was chosen as our calibration case study. We concentrated on calibrating CASC2D for this particular basin using synthetic and storm radar rainfall from the WSI PRECIP product.

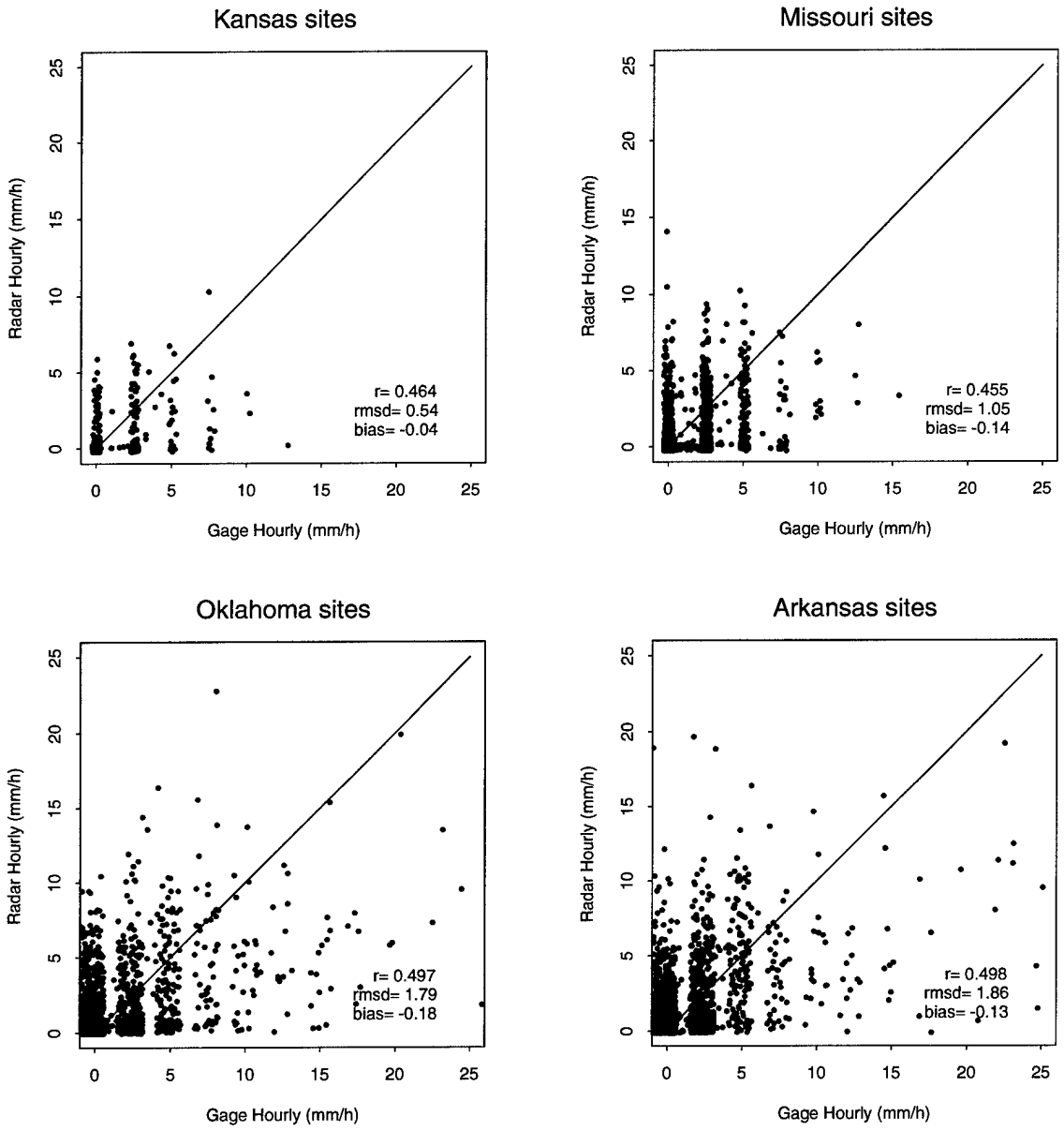

Figure 18: Radar versus rain gauge scatterplots of near-instantaneous rain rate for the storm of 3–8 January 1998.

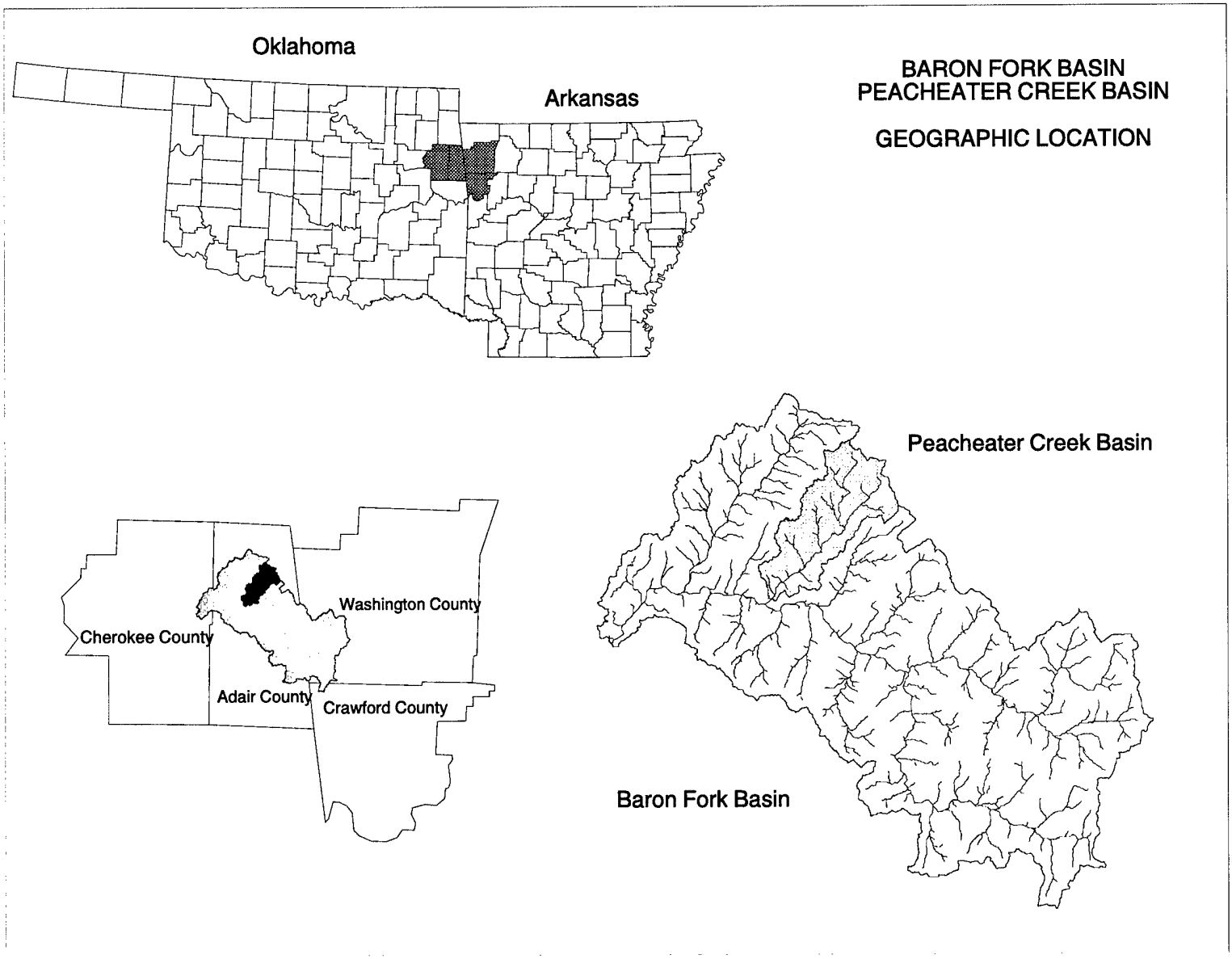

Figure 19: Baron Fork location maps. In the map of Oklahoma and Arkansas, the counties containing the Baron Fork are shaded. These counties are expanded below and identified. In this map the Baron Fork is shaded, and the Peacheater Creek Basin is darker. The map to the right shows the stream network making up the Baron Fork. Here the Peacheater Creek Basin is shaded.

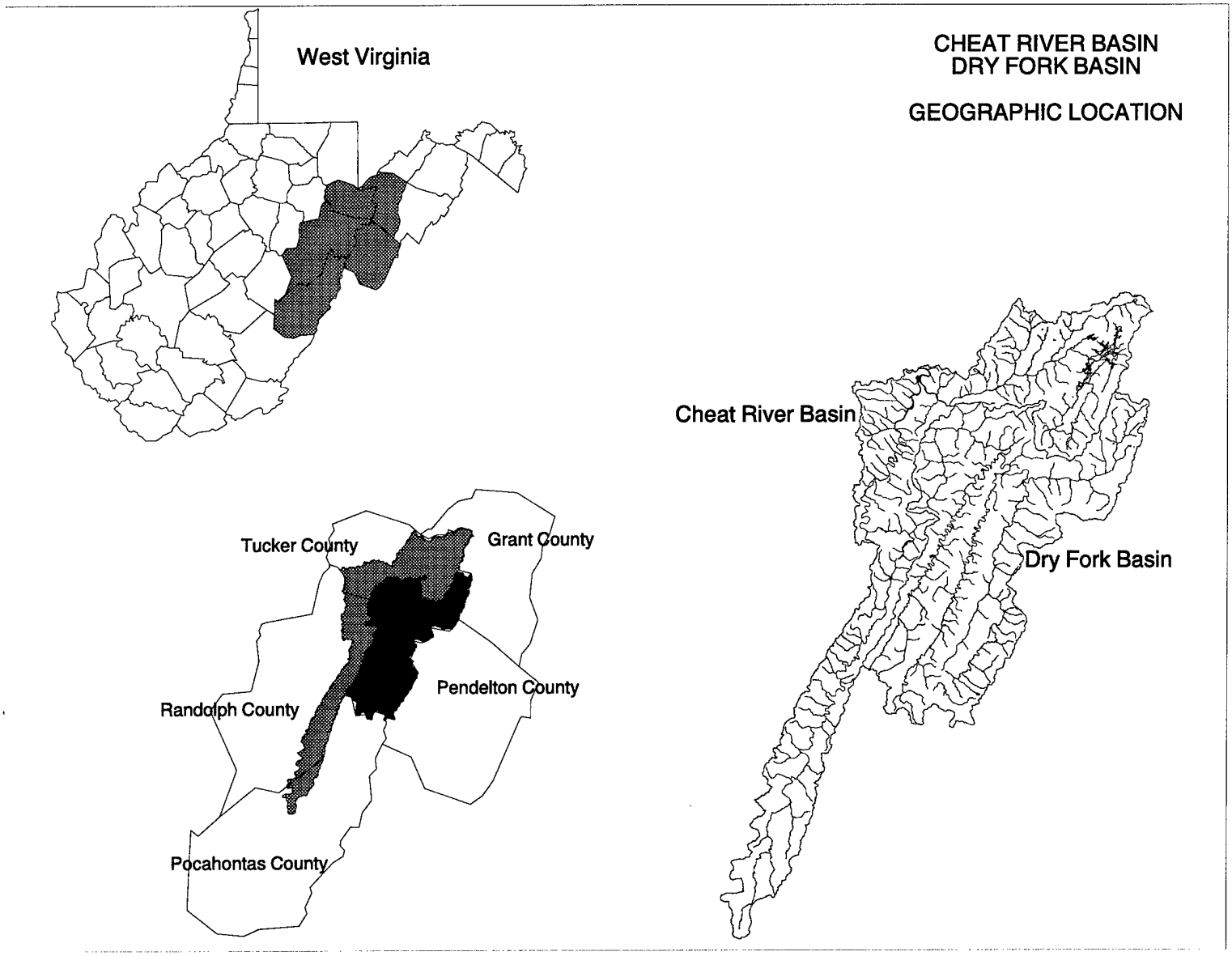

Figure 20: Cheat River location maps. As in Fig. 19 for the Cheat River and Dry Fork.

The required input parameters to CASC2D include topography, soil infiltration characteristics, surface roughness, stream network and channel geometry. Watershed data for the four test basins were abstracted from the available geographical data sources for the CONUS. These data sources included United States Geological Survey (USGS) 7.5 minute Digital Elevation Models (DEM), United States Department of Agriculture-National Resource Conservation Service (USDA-NRCS) State Soil Geographic Survey Data, Land Use Land Cover (LULC) Data and 1995 Topologically Integrated Geographic Encoding and Referencing (TIGER) census Data. In addition, the USGS daily and hourly stream discharge data for all relevant streamflow gauges were compiled. Selected field surveyed channel cross sections were used in estimating stream network geometry (Dutnell 2000, Tortorelli 2000 [11, 48]).

A Geographical Information System (GIS) served as the interface between the relevant data layers (elevation, soils, land use) and the input parameters required by the distributed hydrological model. Data management and manipulation was performed efficiently through a suite of available functions for terrain and hydrological modeling in ARC/INFO and ArcView (ESRI 1999 [13]). GIS modeling allowed for the derivation of hydrologically-corrected DEMs, determination of overland flow directions and accumulations, calculation of terrain slope and aspect and the extraction of the stream networks and watershed boundaries for the four basins. The GIS was used to reclassify the soil texture and land use data to the appropriate infiltration and overland flow parameters required for the hydrological model based upon published relationships (e.g. Rawls *et al.* 1983, Chow 1959 [40, 9]). The results of this task are shown in Fig. 21 and Fig. 22.

The GIS data manipulation and management was coupled to the Watershed Modeling System (WMS) which contains an interface specifically designed to format the raster-based inputs for the CASC2D model. This software package allowed for the creation of the specific stream network files, including the modifications necessary for proper channel routing. It also assists in composing the model run files and checking for potential error sources.

We conducted a thorough test of the CASC2D model sensitivity to input parameters for a simplified synthetic rainfall in the Peacheater Creek basin. We consider this a crucial step in evaluating model performance prior to use of the distributed radar rainfall. The sensitivity to storm duration and intensity, model time step, spatial variation of soil moisture and roughness, channel geometry and stream network density were all tested using a uniform rainfall pattern. Examples of the responses to these synthetic storms are shown in Fig. 23. These sensitivity tests resulted in improved model initialization. In particular, the distributions of three critical parameters were updated in this off-line model calibration: the initial soil moisture, the stream network density and the channel geometry. Initial soil moisture is critical for a surface hydrological model such as CASC2D. An improved representation was obtained using a TOPMODEL approach to ensure spatial heterogeneity in the watershed infiltration response. The channel network density and cross sectional geometry is a major factor in calibrating CASC2D due to the emphasis placed on routing channel flow through the stream network. Various objective approaches were undertaken to obtain the appropriate channel head definition and the geometry was derived using an empirically tuned theoretical

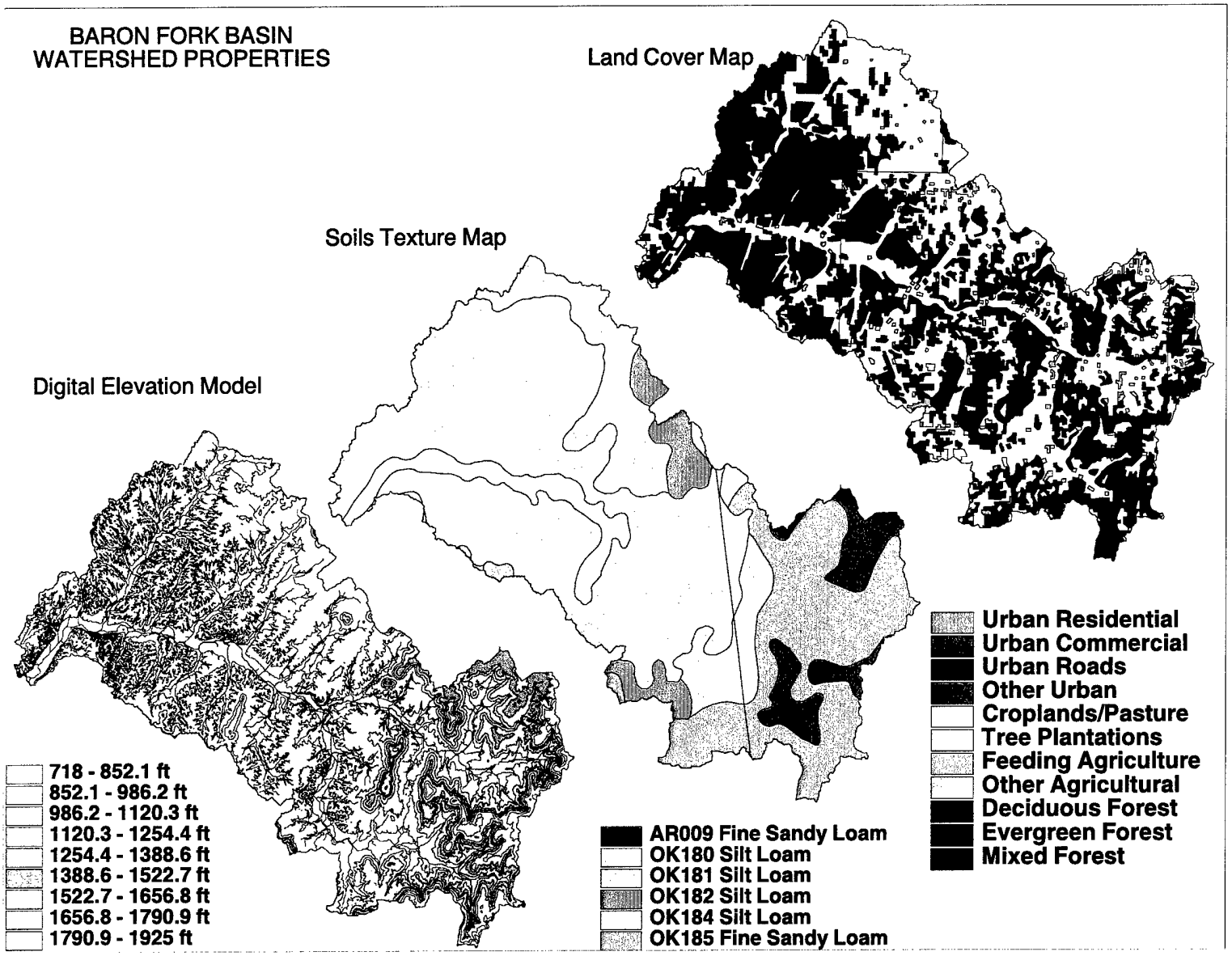

Figure 21: Baron Fork properties maps. CASC2D makes use of detailed maps of elevation, soil texture and land use.

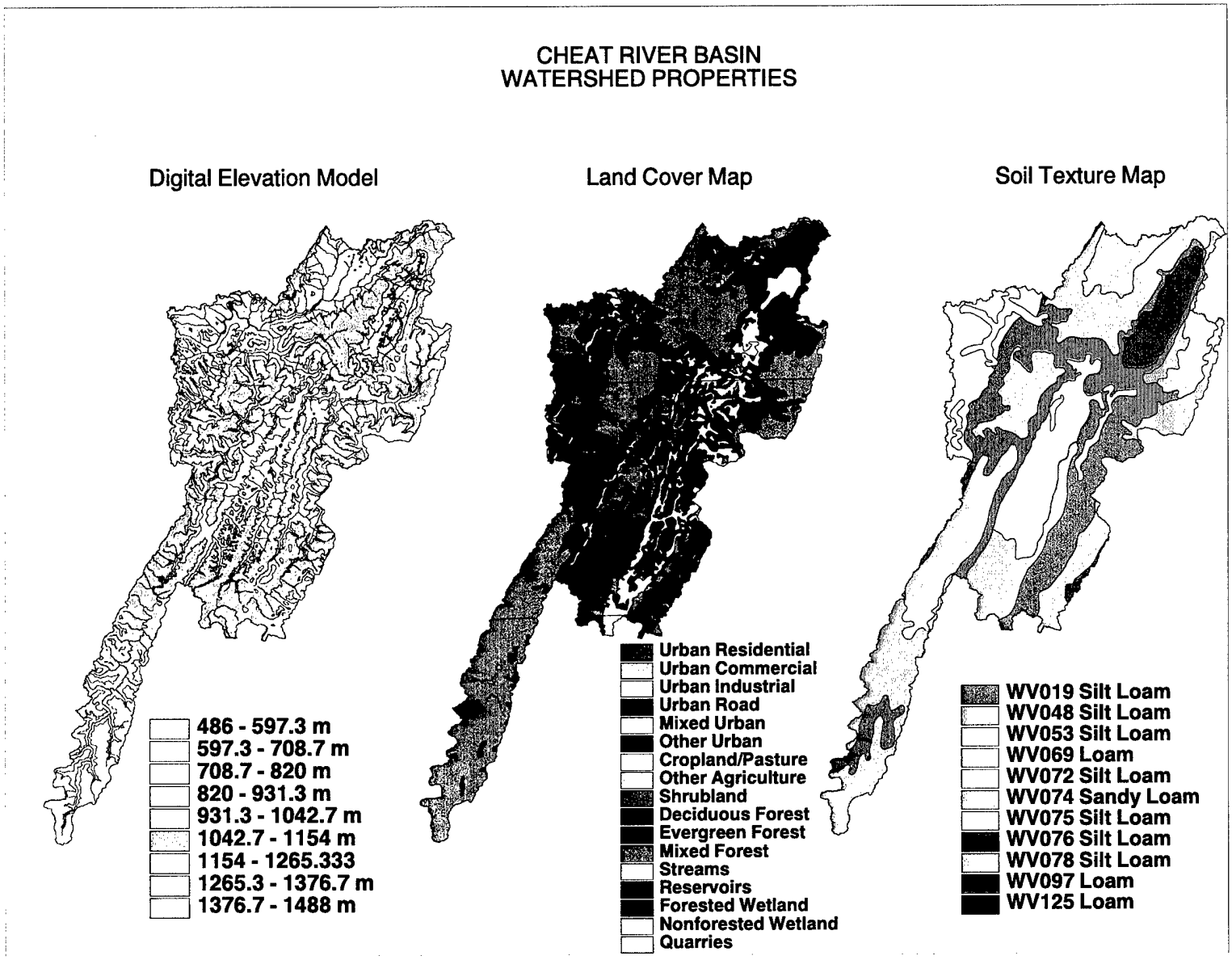

Figure 22: Cheat River properties maps.

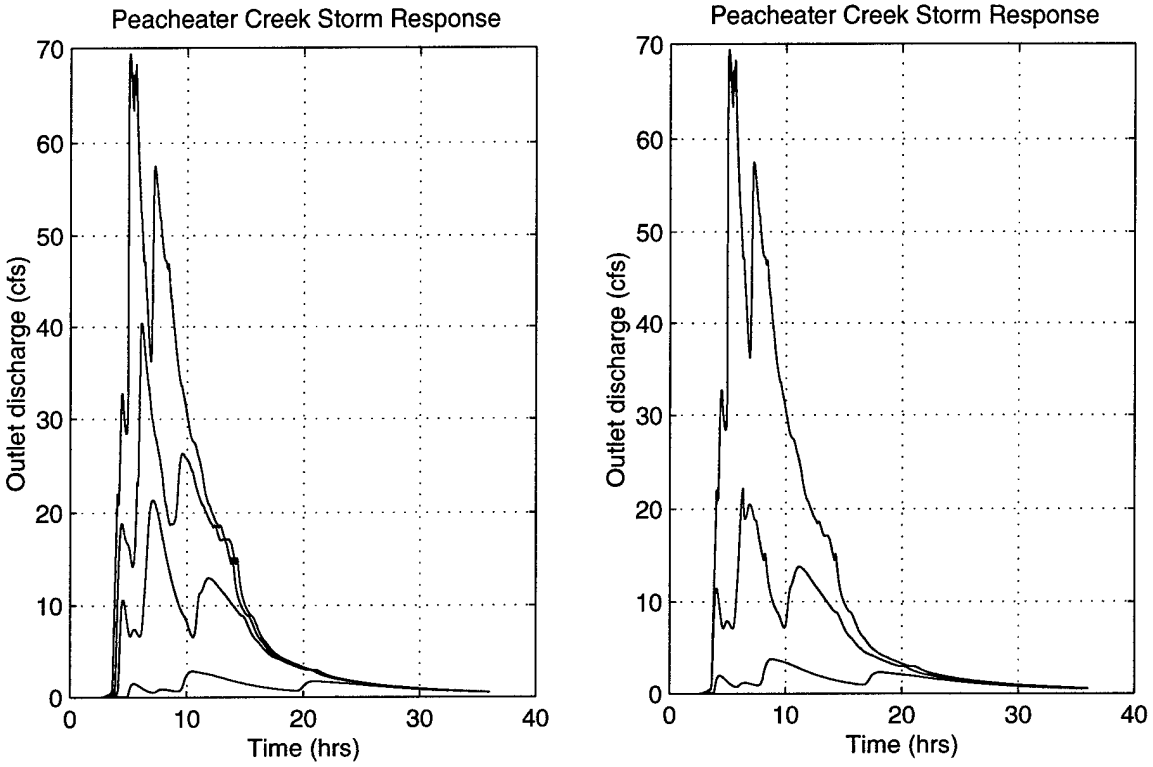

Figure 23: Response to step function storm. On the left are storms of duration 4 hours and intensities of 16, 18, 19 and 20 mm/hr. On the right are storms of 20 mm/hr and 3, 3.5 and 4 hours. (The top most curve is the same case in the two panels.)

model relating channel area to watershed contributing area. These three off-line calibration schemes led to great improvements in model performance. The details of these analyses are discussed in Hoffman *et al.* (2000 [23]).

Based upon the implementation of the synthetic rainfall data for the Peacheater Creek watershed, the most recent portion of the hydrological effort consisted of modeling the response to spatially varied radar rainfall input. Fig. 24 shows the relationship of the radar grid to the basin. By comparing the available streamflow and WSI PRECIP records, various storms were identified for the period of 1996-1999. A storm experiment was setup for one storm (3–8 January 1998) and the baseflow recession analysis performed to obtain the storm runoff over the storm period. The results of this experiment are shown in Fig. 28. The time origin for this figure is 0300 UTC, so that the peak rainfall, plotted along the top of the figure, occured during the 0900 – 2100 UTC period, in agreement with Fig. 8. Calibration of the model parameters based upon the comparison of the outlet hydrograph from the streamflow record and model was then performed in various logical steps following knowledge of the effects of model parameters on the hydrograph response.

Comparisons of the model response and the observed hydrograph for the baseline case (i.e. parameters obtained directly from literature cited values) suggested the need for changes to model parameters that control both runoff volume and peak runoff time. Due to the infiltration scheme used in CASC2D, incident rainfall that does not infiltrate, due to exceedence of an infiltration capacity, becomes overland runoff that is directly routed to the outlet (although reinfiltration can occur along the overland flow path). In order to increase the runoff volume in the model response, the infiltration needed to be reduced by lowering the value of the saturated hydraulic conductivity (K_s in cm/hr). Changes to K_s below the accepted values for the soil type in Peacheater Creek were required in order to match the runoff volume during the calibration tests. Fig. 25 shows two of the calibration tests for K_s based on typical values for silt loam and clay soil types. Using the K_s value ($0.068\ cm/hr$) for clay matched the observed runoff volume despite the fact that the watershed is characterized by a silt loam soil type. This discrepancy is due both to the CASC2D model formulation as an infiltration-excess type model and the generalizations made when assigning a model parameters based on a specific soil type uniformly over the basin.

The runoff volume is also controlled by the antecedent moisture conditions in the watershed. If a large rainfall event occurs over a saturated soil surface, less infiltration will occur and consequently more runoff is expected. By increasing the antecedent soil moisture θ_i uniformly over the basin, an increase in the runoff volume was obtained. Furthermore, a spatially-distributed antecedent moisture conditions was developed through the use of a TOPMODEL approach to wetness and applied as the initial condition. This provided an improved runoff volume computation and a more realistic distribution of wetness over a larger range of possible wetness states in the basin. Results of these sensitivity tests during the calibration phase are shown in Fig. 26.

Once the model runoff volume was comparable to the observations, changes were required to the timing of the peak flow. Testing of the model sensitivity to the overland and channel roughness parameters suggested that runoff peak time was controlled primarily by the

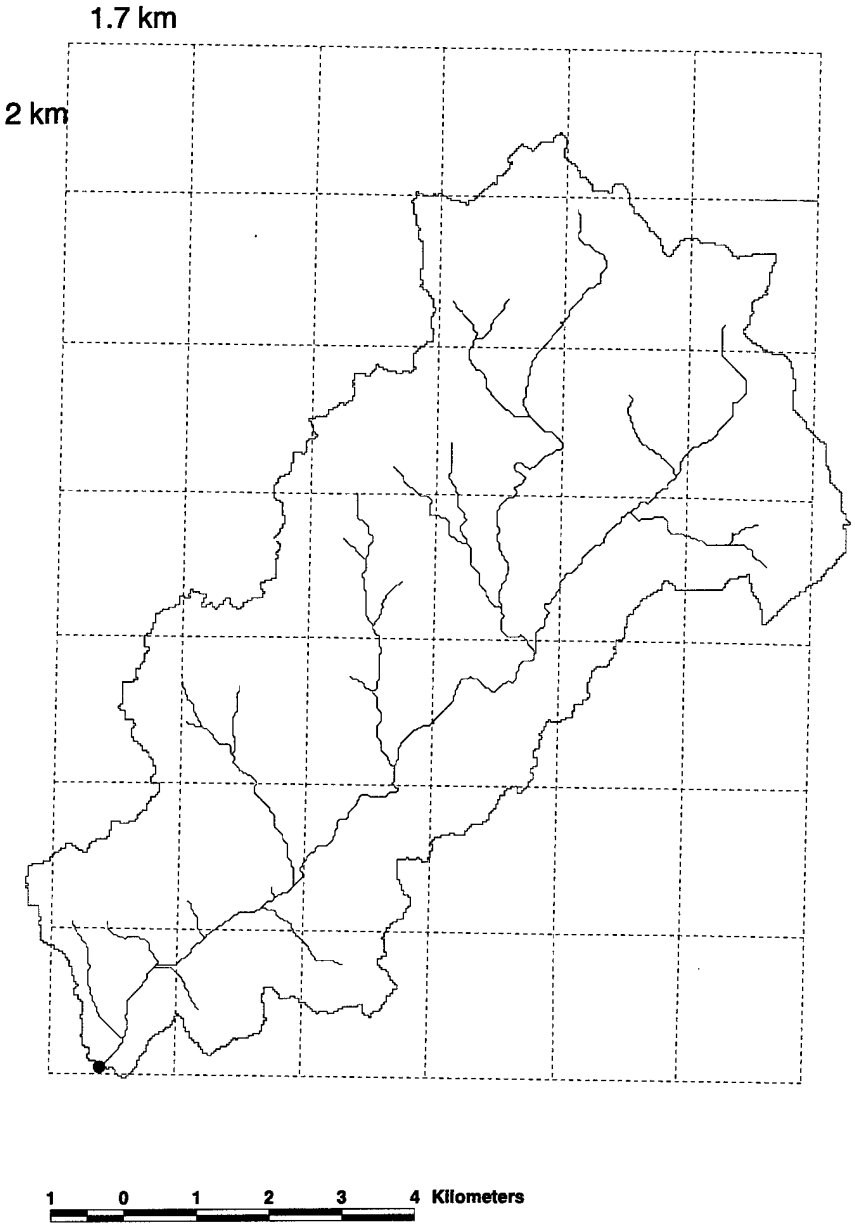

Figure 24: The PRECIP grid in relationship to the Peacheater Creek.

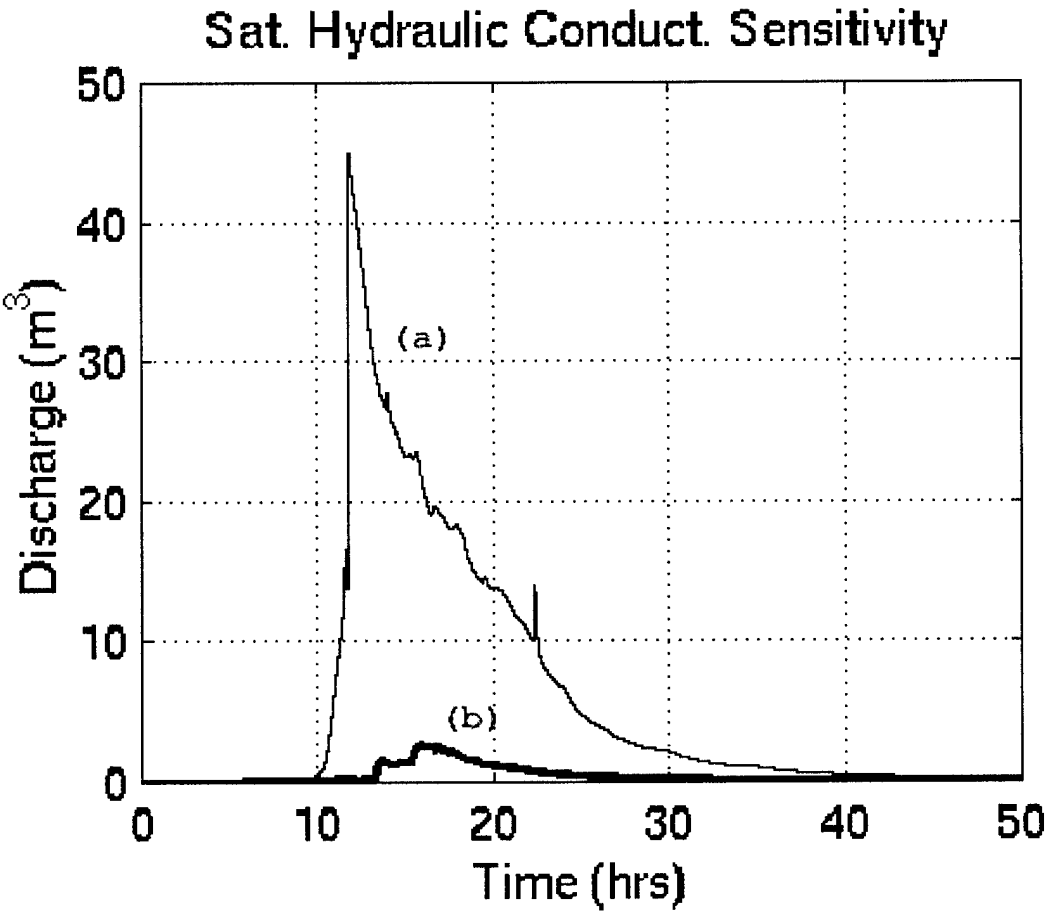

Figure 25: WMS-CASC2D sensitivity and calibration test for a model parameter controlling infiltration under a Green and Ampt scheme: saturated hydraulic conductivity K_s. (a) spatially-uniform $K_s = 0.068\ cm/hr$ for clay textural class (b) spatially-uniform $K_s = 0.68\ cm/hr$ for silt loam textural class (Rawls *et al.* 1983 [40]). Model response is discharge (m^3/s) at the Peacheater Creek stream gauge station for the winter storm event of 3–8 January, 1998.

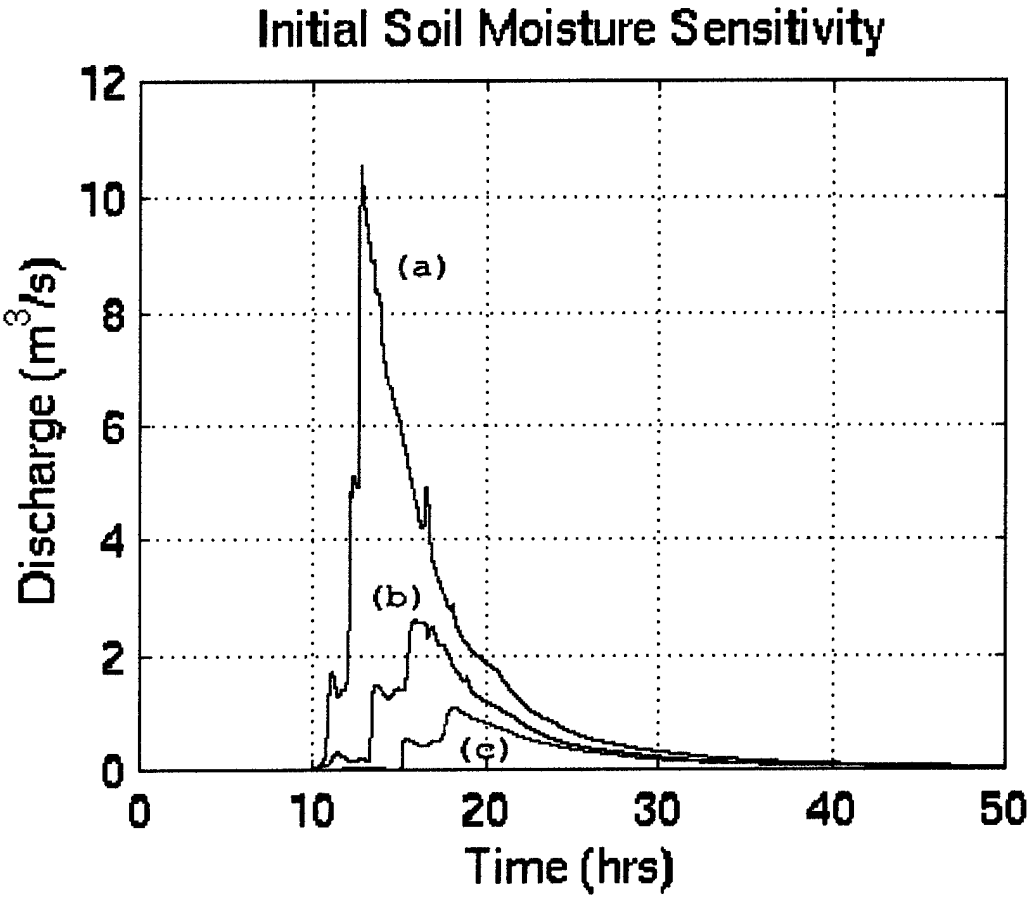

Figure 26: WMS-CASC2D sensitivity and calibration test for a model parameters controlling infiltration: antecendent soil moisture conditions θ_i. (a) spatially-uniform $\theta_i = n_e = 0.486$, where n_e is the effective porosity for silt loam (b) spatially-distributed through TOPMODEL wetness index for range $\theta_i = 0 - n_e$ (c) spatially-uniform $\theta_i = 0.5n_e = 0.243$.

roughness characteristics (Manning n) of the channel routing scheme. Small changes in the Manning n produced significant variations in the modeled hydrograph. The overland Manning n, on the other hand, exhibited a smaller degree of control over the routed hydrograph and also presented problems in the numeric stability of the overland routing scheme. In order to obtain realistic peak runoff times, the Manning n was increased from typical channel values of 0.035 to 0.2, a value associated with channels that contain large obstructions to flow. A reasonable match was obtained with a uniform Manning n of 0.16 over the entire channel network. Fig. 27 shows the high sensitivity that the model hydrograph showed to the Manning n parameter.

By using a trial and error calibration technique on these three important parameters, saturated hydraulic conductivity, antecedent soil moisture and channel roughness coefficient, the model runoff response was able to match sufficiently well the observed hourly hydrograph from the USGS streamgauge. Fig. 28 shows the comparison among the model output and the observed hydrograph for the storm event over the Peacheater Creek Basin. Notice that the rising hydrograph limb is well reproduced, but neither the peak flow rate or recession limb match appropriately. Although, this calibration exercise was not exhaustive (e.g. Senarath *et al.* 2000 [42]), it does demonstrate the sensitivity of the model to particular changes in parameters that control runoff volume and peak timing. In addition, this exercise also shows the limitations of using an infiltration-excess type model for the Peacheater Creek watershed during a winter storm event. To properly reproduce the observed response, values of saturated hydraulic conductivity (K_s) and channel roughness coefficient (n) had to be altered beyond the range of realistic estimates.

The hydrologic modeling results from Phase I were presented at the AGU Spring 2000 meeting in Washington, DC, during a session dedicated to lumped and distributed hydrologic model intercomparisons sponsored by the National Weather Service, Office of Hydrology (Hoffman *et al.* 2000 [23]). Future work during Phase II of the project addresses some of the issues explored during the implementation of CASC2D in the prototype R^{2}FS for the Peacheater Creek Basin in northeastern Oklahoma.

5 Phase II Plans

Our approach for the Rain and River Forecast System (R^{2}FS) is extensible, scalable, and flexible. In our Phase I effort, the initial focus was a robust baseline system consisting of WMS-CASC2D as a hydrologic model and the WSI PRECIP product as our distributed rainfall data source. Enhancements or additional modules may now be replaced or added to refine and to extend the system in a step-by-step process during the latter phases of the project. This approach mitigates risk, providing an early proof of concept operational product at low initial cost, which at the same time provides the basic building blocks for the evolutionary development of the system. The lessons learned during the Phase I effort can be fully integrated into the development plans in Phase II.

Key points for the continued development of R^{2}FS are the following:

Development of spatially-distributed hydrologic model to replace WMS-CASC2D within

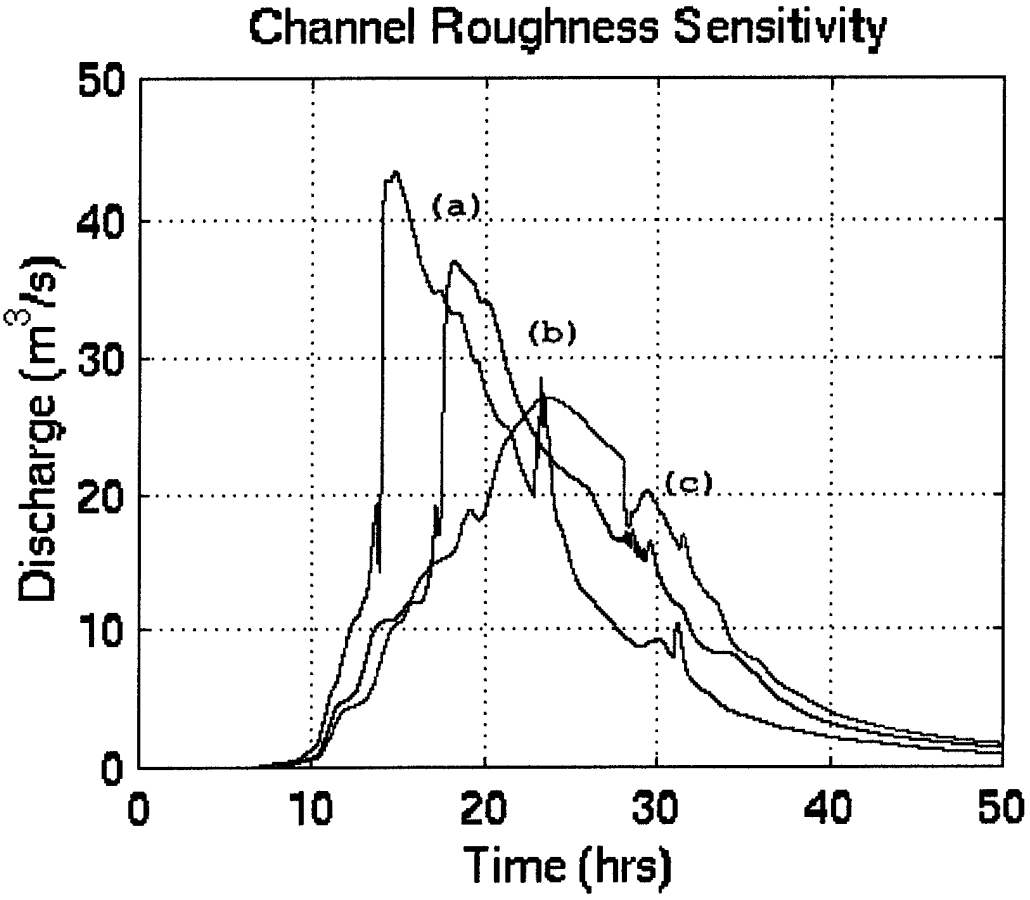

Figure 27: WMS-CASC2D sensitivity and calibration test for a model parameter controlling flood routing: channel roughness coefficient n. (a) spatially-uniform $n = 0.1$ for channel network grid cells (b) $n = 0.16$ and (c) $n = 0.2$. These high roughness values are more characteristic of overland flow than in-channel streamflow (Chow, 1959 [9]). Note the high sensitivity to n in terms of hydrograph translation and attenuation.

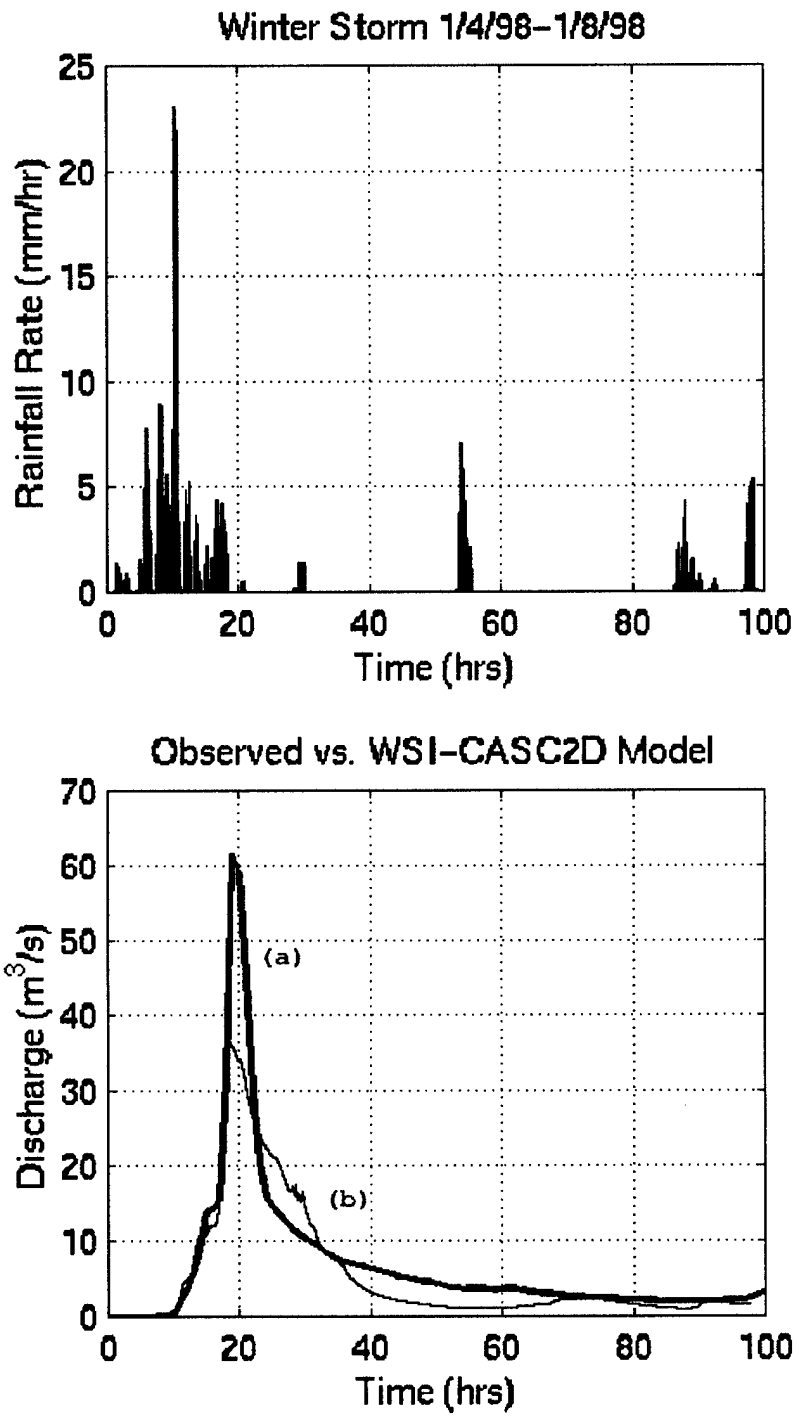

Figure 28: Comparison of WMS-CASC2D calibration with observed streamflow discharge at the Peacheater Creek streamgauge (07196973) in Adair County, OK, for the storm of 3–8 January, 1998. The top panel shows the area-averaged rainfall rate (in mm/hr) over the Peacheater Creek catchment obtained from the WSI PRECIP product. The bottom panel shows the comparison of the observed (a) and modeled streamflow (b) using the calibration parameter set: $K_s = 0.068\ cm/hr$, $\theta_i = 0 - n_e$, $n = 0.16$.

R^2FS. We will use the M.I.T. Parsons hydrological model as a baseline system due to its coupling of unsaturated and saturated zone process dynamics and capability of modeling various runoff generation mechanisms including saturation and infiltration-excess types. Significant modifications to the flow routing scheme will be implemented to allow for a physically-based hydraulic routing in the river network and floodplain. This will permit modeling of the spatially-varied flood response in terms of flow depth, discharge and inundation extent. The new tool will permit novel approaches to distributed model calibration and validation with the use of distributed flood inundation data available from satellite imagery and flood mapping studies. In addition, the model interphase and spatial data analysis capabilities of the M.I.T. Parsons hydrological model will be enhanced by coupling it to a geographic information system, as outlined by Rybarczyk (2000 [41]).

The WSI PRECIP product is our baseline precipitation data source. The PRECIP data have already been validated by Vollrath (1996 [49]), and we have begun to extend his analysis. In the future, refinements and improvements to PRECIP automatically become part of the R^2FS. Note that PRECIP will be used both for data assimilation and for rainfall forecast verification. In later phases of the project, the capability to ingest ground-based and satellite-based precipitation estimates will be added.

The baseline precipitation forecast techniques are three which already exist:

1. Persistence will be implemented as a baseline and a starting point for further refinements.

2. The M.I.T. Lincoln Lab extrapolation method is expected to be our most useful short range technique.

3. Operational Eta forecasts will provide useful longer range techniques.

For forecast blending, we will prototype a simple decision tree blending technique. In practice, this will amount to using the extrapolation forecast until a critical time is reached, and then switching to the Eta (NWP) forecast. At times near the critical time, when multiple forecasts are useful, the decision tree will be refined to blend the individual forecasts. The critical times for changing forecast methods, as well as the relative weights for merging different forecasts, will be determined by verifying each method against PRECIP.

References

[1] R. F. Adler, A. J. Negri, P. R. Keehn, and I. M. Hakkarinen. Estimation of monthly rainfall over Japan and surrounding waters from a combination of low-orbit microwave and geosynchronous IR data. *J. Applied Meteorol.*, 32:335–356, 1993.

[2] E. A. Anderson. Development and testing of snowpack energy balance equations. *Water Resources Research*, 4(1), 1968.

[3] P. A. Arkin. The relationship between fractional coverage of high cloud and rainfall accumulations during GATE over the B-scale array. *Mon. Weather Rev.*, 107:1382–1387, 1979.

[4] P. A. Arkin and B. N. Meisner. The relationship between large-scale convective rainfall and cold cloud over the western hemisphere during 1982-1984. *Mon. Weather Rev.*, 115:51–74, 1987.

[5] A. K. Betts. A new convective adjustment scheme. Part I: Observational and theoretical basis. *Q. J. R. Meteorol. Soc.*, 112:677–691, 1986.

[6] A. K. Betts and M. J. Miller. A new convective adjustment scheme. Part II: Single column tests using GATE wave, BOMEX, ATEX, and Arctic air-mass data sets. *Q. J. R. Meteorol. Soc.*, 112:693–709, 1986.

[7] J. P. Charba and W. H. Klein. Skill in precipitation forecasting in the national weather service. *Bull. Am. Meteorol. Soc.*, 61(12):1546–1555, Dec. 1980.

[8] F. Chen, T. T. Warner, K. Manning, and D. Yates. Using a high-resolution mesoscale coupled model to simulate the 1996 Buffalo Creek flash-flood event. In *15th Conference on Hydrology*, pages 214–217, Long Beach, California, 9–14 Jan. 2000. American Meteorological Society, Boston, MA.

[9] V. T. Chow. *Open Channel Hydraulics.* McGraw-Hill, New York, 1959.

[10] B. A. Colle, K. J. Westrick, and C. F. Mass. Evaluation of MM5 and Eta-10 precipitation forecasts over the Pacific Northwest during the cool season. *Weather Forecast.*, 14(2):137–154, 1999.

[11] R. C. Dutnell. Development of bankfull discharge and channel geometry relationships for natural channel design in Oklahoma using a fluvial geomorphic approach. Master's thesis, Oklahoma University, 2000.

[12] D. Entekhabi and P. S. Eagleson. Land surface hydrology parameterization for atmospheric general circulation models: Inclusion of subgrid scale spatial variability and screening with a simple climate model. Technical Report 325, Ralph M. Parsons Laboratory, Massachusetts Institute of Technology, Cambridge, MA, 1989.

[13] ESRI. *ArcView version 3.1. Arc/Info version 7.2.* Environmental Systems Research Institute, 1999.

[14] R. R. Ferraro and G. F. Marks. The development of SSM/I rain-rate retrieval algorithms using ground-based radar measurements. *J. Atmospheric Oceanic Technology*, 12(4):755–770, Aug. 1995.

[15] A. R. Ganguly, L. Garrote, and R. L. Bras. Application of a physically-based distributed hydrologic model to large basins. In *13th Conference on Hydrology*, Long Beach, CA, 2–7 Feb. 1997. American Meteorological Society, Boston, MA.

[16] L. Garand and C. Grassotti. Towards an objective analysis of rainfall rate combining observations and short-term forecast model estimates. *J. Applied Meteorol.*, 34(9):1962–1977, Sept. 1995.

[17] G. Gong, D. Entekhabi, and G. D. Salvucci. Regional and seasonal estimates of fractional storm coverage based on station precipitation observations. *J. Climate*, 7(10):1495–1505, 1994.

[18] C. Grassotti and L. Garand. Classification-based rainfall estimation using satellite data and numerical forecast model fields. *J. Applied Meteorol.*, 33(2):159–178, 1994.

[19] C. Grassotti, R. N. Hoffman, and H. Iskenderian. Fusion of ground-based radar and satellite-based rainfall data using feature calibration and alignment. *J. Applied Meteorol.*, 38(6):677–695, June 1999.

[20] C. Grassotti, S. M. Leidner, J.-F. Louis, and R. N. Hoffman. Development and application of a visible-infrared rain flag for scatterometer data. *J. Applied Meteorol.*, 38(6):665–676, June 1999.

[21] N. C. Grody. Classification of snow cover and precipitation using the Special Sensor Microwave Imager. *J. Geophys. Res.*, 96(D4):10941–10954, 1991.

[22] R. N. Hoffman and E. Kalnay. Lagged average forecasting, an alternative to Monte Carlo forecasting. *Tellus*, 35A:100–118, 1983.

[23] R. N. Hoffman, D. Entekhabi, C. Grassotti and E. R. Vivoni. Real-Time Distributed Hydrometeorological Forecasting using NEXRAD data. AGU 2000 Spring Meeting, Washington, D. C., 2000. Available online: http://web.mit.edu/vivoni/www/aguspring.html

[24] Z. Janjić. The step-mountain coordinate: Physical package. *Mon. Weather Rev.*, 118(7):1429–1443, 1990.

[25] Z. Janjić. The step-mountain Eta coordinate model: Further developments of the convection, viscous sublayer, and turbulence closure schemes. *Mon. Weather Rev.*, 122(5):927–945, 1994.

[26] J. E. Janowiak. Tropical rainfall: A comparison of satellite derived rainfall estimates with model precipitation forecasts, climatologies, and observations. *Mon. Weather Rev.*, 120:448–462, 1992.

[27] C. Kummerow, R. A. Mack, and I. M. Hakkarinen. A self-consistency approach to improve microwave rainfall rate estimation from space. *J. Applied Meteorol.*, 28:869–884, 1989.

[28] C. Kummerow, W. S. Olson, and L. Giglio. A simplified scheme for obtaining precipitation and vertical hydrometeor profiles from passive microwave sensors. *IEEE Trans. Geosci. Remote Sens.*, 34(5):1213–, Sept. 1996.

[29] G. Liu and J. A. Curry. Retrieval of precipitation from satellite microwave measurement using both emission and scattering. *J. Geophys. Res.*, 97(D9):9959–9974, 1992.

[30] F. Mesinger. Improvements in quantitative precipitation forecasts with the Eta regional emodel at the National Centers for Environmental Prediction: The 48-km upgrade. *Bull. Am. Meteorol. Soc.*, 77(11):2637–2649, Nov. 1996.

[31] D. G. Morris. A categorical, event oriented, flood forecast verification system for the national weather service. Technical Memorandum HYDRO-43, NOAA, Washington, DC, 1988.

[32] A. H. Murphy and R. L. Winkler. A general framework for forecast verification. *Mon. Weather Rev.*, 115(7):1330–1338, 1987.

[33] T. Nehrkorn, M. Mickelson, L. W. Knowlton, and M. Živković. A global forecast model comparison study – year 1. Technical Report 93-2203, Phillips Laboratory, Hanscom AFB, MA, 1993.

[34] NRC. *Towards a New National Weather Service: Assessment of Hydrologic and Hydrometeorological Operations and Services.* National Research Council, Commission on Engineering and Technical Systems, National Weather Service Modernization Committee, Washington, DC, 1996.

[35] W. S. Olson. Physical retrieval of rainfall rates over the ocean by multispectral microwave radiometry: Application to tropical cyclones. *J. Geophys. Res.*, 94(D2):2267–2280, 1989.

[36] W. S. Olson, C. Kummerow, G. M. Heymsfield, and L. Giglio. A method for combined passive-active microwave retrievals of cloud and precipitation profiles. *J. Applied Meteorol.*, 35(8):1763–1789, 1996.

[37] W. S. Olson and C. D. Kummerow. Simulated retrieval of precipitation profiles from TRMM microwave imager and precipitation radar data. In *Eighth Conference on Satellite Meteorology and Oceanography*, pages 248–251, Atlanta, Georgia, 28 Jan.–2 Feb. 1996. American Meteorological Society, Boston, MA.

[38] S. Perica and E. Foufoula-Georgiou. A model for multi-scale disaggregation of spatial rainfall based on coupling meteorological and scaling descriptions. *J. Geophys. Res.*, 101(D3):26347–26361, 1996.

[39] G. W. Petty. Physical retrievals of over-ocean rain rate from multichannel microwave imagery. Part II: Algorithm implementation. *Meteorol. Atmos. Phys.*, 54:101–122, 1994.

[40] W. J. Rawls, D. L. Brakensiek, and N. Miller. Green-Ampt infiltration parameters from soils data. *J. Hydraulic Engineering*, 109(1):62–70, 1983.

[41] S. M. Rybarcyzk. Formulation and Testinf of a distributed, triangular irregular network, rainfall/runoff model. M. S. Thesis, Massachusetts Institute of Technology, 185 pgs, 2000.

[42] S. U. S. Senarath, F. L. Ogden, C. W. Downer and H. O. Sharif. On the calibration and verification of two-dimensional, distributed, Hortonian, continuous watershed models. *Water Resources Research*, 36(6): 1495-1510, 2000.

[43] J. A. Simpson, R. F. Adler, and G. R. North. A proposed tropical rainfall measuring mission (TRMM) satellite. *Bull. Am. Meteorol. Soc.*, 69:278–295, 1988.

[44] E. A. Smith, J. E. Lamm, R. Adler, J. Alishouse, K. Aonashi, E. Barrett, P. Bauer, W. Berg, A. Chang, R. Ferraro, J. Ferriday, S. Goodman, N. Grody, C. Kidd, D. Kniveton, C. Kummerow, G. Liu, F. Marzano, A. Mugnai, W. Olson, G. Petty, A. Shibata, R. Spencer, F. Wentz, T. Wilheit, and E. Zipser. Results of WetNet PIP-2 project. *J. Atmospheric Sciences*, 55(9):1483–1536, 1 May 1998.

[45] R. W. Spencer. A satellite passive 37-GHz scattering-based method for measuring oceanic rain rates. *J. Climate Appl. Meteorol.*, 25:754–766, 1986.

[46] H. Sundqvist. A parameterization scheme for non-convective condensation including prediction of cloud water content. *Q. J. R. Meteorol. Soc.*, 104:677–690, 1978.

[47] D. G. Tarboton, T. H. Jackson, J. Z. Liu, C. M. U. Neale, K. R. Cooley, and J. J. McDonnell. A grid based distributed hydrologic model: Testing against data from Reynolds Creek experimental watershed. In *Conference on Hydrology*, pages 79–84, Dallas, TX, 16–20 Jan. 1995. American Meteorological Society, Boston, MA.

[48] B. Tortorelli. pers. comm. USGS Surface Water Specialist. Oklahoma City District Office, 2000.

[49] S. J. Vollrath. A seasonal and regional evaluation of a value-added national radar data set for precipitation. Master's thesis, Massachusetts Institute of Technology, Cambridge, MA, 1996.

[50] M. S. Wigmosta, L. W. Vail, and D. P. Lettenmaier. A distributed hydrology-vegetation model for complex terrain. *Water Resources Research*, 30(6), 1994.

[51] T. T. Wilheit and A. T. C. Chang. An algorithm for retrieval of ocean surface and atmospheric parameters from the observations of the Scanning Multichannel Microwave Radiometer. *Radio Sci.*, 15:525–544, 1980.

[52] M. M. Wolfson, B. E. Forman, R. G. Hallowell, and M. P. Moore. The growth and decay storm tracker. In *Eighth Conference on Aviation, Range and Aerospace Meteorology*, pages 58–62, Dallas, Texas, 10-15 Jan. 1999. American Meteorological Society, Boston, MA.

[53] Z. Yu, M. N. Lakhtakia, and E. J. Barron. Modeling the river-basin response to single-storm events simulated by a mesoscale meteorological model at various resolutions. *J. Geophys. Res.*, 104(D16):19675–19689, 27 Aug. 1999.

[54] S. Zhang and E. Foufoula-Georgiou. Subgrid-scale rainfall variability and its effects on atmospheric and surface variable predictions. *J. Geophys. Res.*, 102(D16):19559 – 19573, 1997.

[55] Q. Zhao, T. L. Black, and M. E. Baldwin. Implementation of the cloud prediction scheme in the Eta model at NCEP. *Weather Forecast.*, 12:697–712, 1997.

[56] E. Zipser. Rainfall predictability: When will extrapolation-based algorithms fail? In *Eighth Conference on Hydrometeorology*, pages 138–142, Alberta, Canada, 1990. AMS+.

A WSI SPECIAL data holdings

For each calendar day we list the number of files per day. A complete day would have a count of 96.

1997

	Jan	Feb	Mar	Apr	May	Jun	Jul	Aug	Sep	Oct	Nov	Dec
1	--	--	--	--	--	--	--	--	--	--	--	96
2	--	--	--	--	--	--	--	--	--	--	--	96
3	--	--	--	--	--	--	--	--	--	--	--	96
4	--	--	--	--	--	--	--	--	--	--	--	58
5	--	--	--	--	--	--	--	--	--	--	--	93
6	--	--	--	--	--	--	--	--	--	--	--	93
7	--	--	--	--	--	--	--	--	--	--	--	96
8	--	--	--	--	--	--	--	--	--	--	--	96
9	--	--	--	--	--	--	--	--	--	--	--	95
10	--	--	--	--	--	--	--	--	--	--	--	96
11	--	--	--	--	--	--	--	--	--	--	--	96
12	--	--	--	--	--	--	--	--	--	--	--	96
13	--	--	--	--	--	--	--	--	--	--	--	94
14	--	--	--	--	--	--	--	--	--	--	--	95
15	--	--	--	--	--	--	--	--	--	--	--	96
16	--	--	--	--	--	--	--	--	--	--	--	96
17	--	--	--	--	--	--	--	--	--	--	96	96
18	--	--	--	--	--	--	--	--	--	--	34	96
19	--	--	--	--	--	--	--	--	--	--	96	96
20	--	--	--	--	--	--	--	--	--	--	90	93
21	--	--	--	--	--	--	--	--	--	--	96	96
22	--	--	--	--	--	--	--	--	--	--	92	95
23	--	--	--	--	--	--	--	--	--	--	64	--
24	--	--	--	--	--	--	--	--	--	--	25	37
25	--	--	--	--	--	--	--	--	--	--	96	96
26	--	--	--	--	--	--	--	--	--	--	96	96
27	--	--	--	--	--	--	--	--	--	--	96	96
28	--	--	--	--	--	--	--	--	--	--	95	96
29	--	--	--	--	--	--	--	--	--	--	96	95
30	--	--	--	--	--	--	--	--	--	--	95	95
31	--	--	--	--	--	--	--	--	--	--	--	92

1998

	Jan	Feb	Mar	Apr	May	Jun	Jul	Aug	Sep	Oct	Nov	Dec
1	95	95	96	--	70	43	--	--	--	--	--	--
2	96	95	96	--	--	95	--	--	--	--	--	--
3	95	95	96	--	--	96	87	--	--	--	--	--
4	96	95	77	--	43	48	93	--	--	--	--	--
5	75	96	90	--	96	89	7	--	--	--	--	--
6	92	92	31	--	95	93	34	--	--	--	--	--
7	96	88	90	--	96	80	96	--	--	--	--	--
8	91	--	95	--	94	96	96	--	--	--	--	--
9	94	95	70	--	96	96	96	--	--	--	--	--
10	94	96	95	--	96	70	94	--	--	--	--	--
11	95	96	96	--	91	42	88	--	--	--	--	--
12	96	96	95	--	72	93	87	--	--	--	--	--
13	95	95	81	96	34	76	26	--	--	--	--	--
14	96	94	--	96	80	30	96	--	--	--	--	--
15	96	96	--	96	84	82	96	--	--	--	--	--
16	96	96	38	95	94	83	96	--	--	--	--	--
17	95	94	96	95	96	71	96	--	--	--	--	--
18	96	95	46	--	95	96	96	--	--	--	--	--
19	95	95	95	--	89	93	92	--	--	--	--	--
20	96	95	95	--	--	94	83	--	--	--	--	--
21	96	93	95	34	--	96	96	--	--	--	--	--
22	96	91	96	95	--	94	93	--	--	--	--	--
23	96	96	96	91	--	96	--	--	--	--	--	--
24	96	95	96	--	--	96	--	--	--	--	--	--
25	95	95	--	--	--	95	--	--	--	--	--	--
26	96	96	--	--	--	96	--	--	--	--	--	--
27	96	95	--	--	--	94	--	--	--	--	--	--
28	96	94	--	--	24	95	--	--	--	--	--	--
29	96	--	--	13	95	87	--	--	--	--	--	--
30	77	--	--	95	94	--	--	--	--	--	--	--
31	95	--	--	--	47	--	--	--	--	--	--	--

1999

	Jan	Feb	Mar	Apr	May	Jun	Jul	Aug	Sep	Oct	Nov	Dec
1	--	--	--	--	--	--	96	--	--	--	96	96
2	--	--	--	--	--	96	96	--	--	--	96	95
3	--	--	--	--	--	96	96	--	--	--	95	57
4	--	--	--	--	--	96	--	--	--	--	86	--
5	--	--	--	--	--	96	--	--	--	--	48	--
6	--	--	--	--	--	96	--	--	--	--	48	--
7	--	--	--	--	--	--	--	--	--	--	8	44
8	--	--	--	--	--	--	--	--	--	--	35	96
9	--	--	--	--	--	--	--	--	--	--	47	96
10	--	--	--	--	--	--	--	--	--	--	64	96
11	--	--	--	--	--	--	--	--	--	--	96	96
12	--	--	--	--	--	--	--	--	--	--	96	96
13	--	--	--	--	--	--	--	--	--	--	95	96
14	--	--	--	--	--	--	--	--	--	37	96	96
15	--	--	--	--	--	--	--	--	--	96	96	96
16	--	--	--	--	--	--	--	--	--	94	96	95
17	--	--	--	--	--	--	--	--	--	96	96	89
18	--	--	--	--	--	--	--	--	--	86	96	--
19	--	--	--	--	--	--	--	--	--	--	96	96
20	--	--	--	--	--	--	--	--	--	--	95	96
21	--	--	--	--	--	35	--	--	--	--	96	96
22	--	--	--	--	--	96	--	--	--	--	96	96
23	--	--	--	--	--	96	--	--	--	--	96	96
24	--	--	--	--	--	96	--	--	--	--	96	96
25	--	--	--	--	--	96	--	--	--	--	96	96
26	--	--	--	--	96	96	--	--	--	--	96	96
27	--	--	--	--	--	96	--	--	--	--	55	96
28	--	--	--	--	--	96	--	--	--	--	--	96
29	--	--	--	--	--	96	--	--	--	32	23	96
30	--	--	--	--	--	96	--	--	--	96	83	96
31	--	--	--	--	96	--	--	--	--	96	--	96

2000

	Jan	Feb	Mar	Apr	May	Jun	Jul	Aug	Sep	Oct	Nov	Dec
1	95	96	96	96	96	96	96	96	96	--	--	--
2	96	96	96	96	96	95	96	96	65	--	--	--
3	95	96	96	96	96	96	96	96	75	--	--	--
4	92	96	96	96	96	96	96	96	70	--	--	--
5	94	96	96	95	96	96	96	96	83	--	--	--
6	96	96	96	96	96	96	96	96	96	--	--	--
7	96	96	96	96	96	96	96	95	96	--	--	--
8	95	96	96	96	96	96	96	96	96	--	--	--
9	96	96	96	96	96	96	96	96	96	--	--	--
10	96	96	96	96	95	96	96	96	95	--	--	--
11	96	96	96	96	95	96	96	96	--	--	--	--
12	95	96	96	96	96	96	96	96	--	--	--	--
13	96	96	96	96	96	96	95	96	--	--	--	--
14	96	96	96	96	96	96	96	94	--	--	--	--
15	96	95	96	96	96	96	93	96	--	--	--	--
16	96	96	96	96	96	93	96	95	--	--	--	--
17	96	96	96	96	96	95	96	96	--	--	--	--
18	92	96	95	96	96	95	90	96	--	--	--	--
19	96	96	96	96	96	96	96	96	--	--	--	--
20	96	96	96	96	96	96	96	96	--	--	--	--
21	96	96	96	95	48	96	96	94	--	--	--	--
22	96	96	96	96	96	96	96	96	--	--	--	--
23	96	96	96	96	96	96	96	96	--	--	--	--
24	96	96	96	96	96	96	96	96	--	--	--	--
25	96	96	96	96	96	96	96	96	--	--	--	--
26	96	96	96	96	96	96	95	96	--	--	--	--
27	96	96	95	89	96	94	96	96	--	--	--	--
28	96	48	96	96	96	96	95	96	--	--	--	--
29	96	24	96	96	95	95	95	96	--	--	--	--
30	96	--	96	96	96	96	94	96	--	--	--	--
31	96	--	96	--	96	--	91	96	--	--	--	--

Created 11 September 2000.